

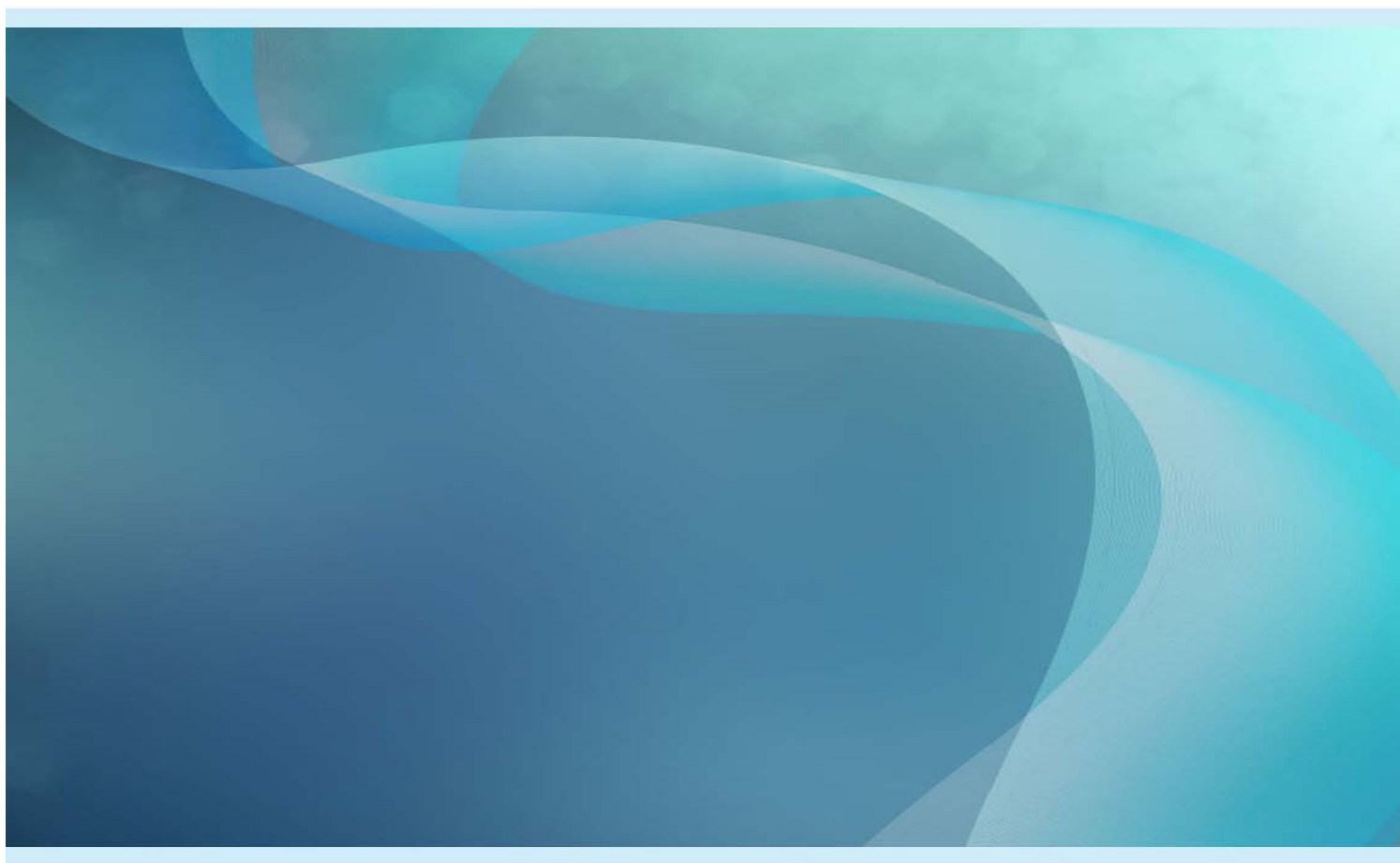


Australian Government
Bureau of Meteorology

Sources of soil dryness measures and forecasts for fire danger rating

Vinod Kumar and Imtiaz Dharssi

December 2015



Sources of soil dryness measures and forecasts for fire danger rating

Vinod Kumar and Imtiaz Dharssi

Bureau Research Report No. 009

December 2015

National Library of Australia Cataloguing-in-Publication entry

Author: Vinod Kumar and Imtiaz Dharssi

Title: Sources of soil dryness measures and forecasts for fire danger rating

ISBN: 978-0-642-70672-0

Series: Bureau Research Report - BRR009

Enquiries should be addressed to:

Vinod Kumar:

Bureau of Meteorology
GPO Box 1289, Melbourne
Victoria 3001, Australia

Contact Email: v.kumar2@bom.gov.au

Copyright and Disclaimer

© 2015 Bureau of Meteorology. To the extent permitted by law, all rights are reserved and no part of this publication covered by copyright may be reproduced or copied in any form or by any means except with the written permission of the Bureau of Meteorology.

The Bureau of Meteorology advise that the information contained in this publication comprises general statements based on scientific research. The reader is advised and needs to be aware that such information may be incomplete or unable to be used in any specific situation. No reliance or actions must therefore be made on that information without seeking prior expert professional, scientific and technical advice. To the extent permitted by law and the Bureau of Meteorology (including each of its employees and consultants) excludes all liability to any person for any consequences, including but not limited to all losses, damages, costs, expenses and any other compensation, arising directly or indirectly from using this publication (in part or in whole) and any information or material contained in it.

Contents

1.	ABSTRACT	1
2.	INTRODUCTION	1
3.	ESTIMATING SOIL MOISTURE DEFICIT USING INDICES BASED ON METEOROLOGICAL PARAMETERS	2
3.1	Keetch–Byram Drought Index (KBDI)	3
3.2	Mount’s Soil Dryness Index (SDI)	4
3.3	Other indices in use internationally	7
4.	<i>IN SITU</i> SOIL MOISTURE OBSERVATIONS	9
4.1	OzNet	11
4.2	CosmOz	11
5.	REMOTE SENSING OF SOIL MOISTURE	12
5.1	SMMR	13
5.2	SSM/I	13
5.3	WindSat	14
5.4	TRMM	14
5.5	ERS	15
5.6	AMSR-E	16
5.7	SMOS & ASCAT	17
5.8	AMSR2	19
5.9	Recent / future platforms	19
6.	LANDSCAPE WATER BALANCE MODELS	20
7.	LAND SURFACE MODELS	21
7.1	LSM inputs	23
7.2	Land surface data assimilation	27
8.	CONCLUSIONS	29
	ACKNOWLEDGMENTS	30
	REFERENCES	31
	APPENDIX A: Theoretical background on microwave remote sensing	39

List of Tables

Table 1	Vegetation classes and corresponding parameter values from Mount (1972).....	5
Table 2	Validation studies of sensors against the <i>in situ</i> observations.	15
Table 3	Generic meteorological forcing variables required to drive an LSM.	25
Table 4	Generic ancillary data required by an LSM	26

List of Figures

Fig. 1	KBDI for 22 nd September 2014 generated at 0.05° resolution using the gridded AWAP rainfall and temperature data.	4
Fig. 2	Same as Fig. 1, but for SDI.	6
Fig. 3	Site locations of (a) OzNet and (b) CosmOz network. Spatial extent of (a) corresponds to the shaded area in its inset. The filled contours represent surface elevation (m) at 10 km resolution.	10
Fig. 4	Overview of soil moisture remote sensing from space – missions and their timelines. Courtesy: <i>European Space Agency and Technische Universität Wien</i>	14
Fig. 5	Three-day (4 – 6 October 2014) averaged maps of retrieved (a) soil wetness index from ASCAT and (b) volumetric soil moisture content from SMOS satellite over Australia.	18
Fig. 6	Volumetric soil moisture content at layers (a) 0.0 – 0.1 m, (b) 0.1 – 0.35 m, (c) 0.35 – 1.0 m, and (d) 1.0 – 3.0 m from the JULES LSM which is coupled to the regional ACCESS numerical weather prediction model. The model resolution is 12 km x 12 km. 23	
Fig. 7	Skill improvement from assimilating either ASCAT or AMSR-E for (a) surface and (b) root-zone soil moisture, as a function of the open-loop and observation skill. The results show that assimilation can improve skill, provided the observation skill minus open-loop skill > -0.2. Skill is defined as the temporal correlation against ground based observations. Courtesy: <i>Draper et al. (2012)</i>	29

1. ABSTRACT

The fuel availability estimates in McArthur Forest Fire Danger Index used in Australia for issuing operational fire warnings is based on soil moisture deficit, calculated as either the Keetch–Byram Drought Index (KBDI) or Mount’s Soil Dryness Index (MSDI). These indices are essentially simplified, empirical water balance models designed to estimate soil moisture depletion in the upper soil levels. These two models over-simplify processes like evapotranspiration and runoff which can lead to large uncertainties in the predicted soil moisture deficit. With advancements in the science of soil moisture measurement and modelling, better products are available for use in fire danger ratings. As such, a detailed review of the established and emerging soil moisture estimation techniques becomes necessary. With this in view, efforts have been made in this paper to discuss various soil moisture estimation methods, their advantages and limitations in a fire danger rating context. The discussion is not intended to be complete and reflect the authors’ interests, but we hope that it helps to highlight the soil moisture data sources that may not be well known outside the hydrological community, especially the people in fire management.

2. INTRODUCTION

Fire danger rating systems are devised to evaluate and integrate the individual and combined factors influencing fire danger. Most of the fire danger rating systems (FDRS) employed in different countries across the world are based on meteorological variables and fuel conditions and give information on the probability of forest fire ignition, propagation and spread. The ignition, spread as well as the short temporal variations in fire danger depend on fuel availability, fuel moisture content (FMC) and prevalent weather conditions (Chandler *et al.*, 1983). FMC is defined as the mass of water contained within the fuel, expressed as percentage of oven-dry mass of that fuel. FMC is a critical variable affecting fire interactions with fuel and partly controls the efficiency of fire ignition and burning. For example, Dowdy and Mills (2012) showed that FMC influences the risk of ignition from lightning in south-east Australia. Fuel availability is the proportion of fuel which will burn in a fire (Luke and McArthur, 1978). Because fuel moisture and fuel availability measures are not always readily available, fire danger rating systems include sub-models to estimate these quantities from weather observations. The McArthur Forest Fire Danger Index (FFDI; McArthur, 1967) used in Australia for instance, has a component representing fuel availability called the Drought Factor, which in turn is partly based on soil moisture deficit

commonly calculated as either the Keetch–Byram Drought Index (KBDI; Keetch and Byram, 1968) or Mount’s Soil Dryness Index (SDI; Mount, 1972).

The soil moisture deficit therefore becomes a key variable in the FFDI calculations done operationally by Bureau of Meteorology in Australia. Accurate estimates and forecasts of soil moisture are therefore crucial to do effective fire danger calculations for wildfire management, rating and warning. Further, it is shown that (Gellie, 2010) the occurrence of large destructive fires corresponds to very large soil moisture deficit values in Australian landscapes, thereby potentially increasing the availability and resulting flammability of the forest fuel structures.

With recent progresses in the science of soil moisture, new products are available which could potentially provide significantly improved accuracy of the soil moisture fields needed for fire danger rating. Also, there are a variety of soil moisture estimation methods used across the world for the application in fire danger rating. This report describes some of the important sources of soil moisture that are established or are emerging, and which can be potentially used in the Australian fire danger rating system. This study intends to be of a preliminary nature to the research that will be carried out to deliver better soil dryness products with greater accuracy at a much higher spatial and temporal resolution for use in operational fire danger rating.

3. ESTIMATING SOIL MOISTURE DEFICIT USING INDICES BASED ON METEOROLOGICAL PARAMETERS

Fuel moisture content is usually divided into dead (DFMC) and live (LFMC) components. LFMC is much more difficult to estimate than DFMC, because it is governed by the complex processes of root water uptake and transpiration that are controlled by multiple physical and biological factors. An accurate estimation of LFMC can be physically measured by the oven-drying of plants (Allen, 1989). This method is simple and reliable but very slow and labour intensive. A regional LFMC assessment is not feasible using this method. Therefore, it is desirable to have models that could reasonably predict the LFMC from more easily accessible parameters. The soil moisture state is a key factor in assessing the dryness of live vegetation due to the correlation that exists between the two variables (Burgan, 1988; Viegas *et al.*, 1992). Given the dependence of FMC on soil moisture, it is convenient to develop mathematical relationships between the two. The KBDI is such a model which measure cumulative soil water deficit in forested ecosystems and is used in Australia as part of the operational fire danger ratings. Studies show that KBDI exhibits a strong relationship

with LFMC (Dimitrakopoulos and Bemmerzouk, 2003). There are a variety of indices in use across the world which uses soil moisture as a proxy and can be related to LFMC. For example, Viegas *et al.* (2001) and Castro *et al.* (2003) found that a non-linear relationships can be derived between moisture codes in the Canadian Forest Fire Weather Index (FWI) system and LFMC data for Mediterranean vegetation. The SDI, which too is a measure of soil moisture deficit, is another method which relates vegetation water stress to soil moisture content and is also used in Australia for fire danger ratings. The following sections give a detailed description of the two methods (KBDI and SDI) used currently in Australia and also provides a short description on other methods used worldwide.

3.1 Keetch–Byram Drought Index (KBDI)

The KBDI is conceptually a cumulative estimate of soil moisture deficit calculated using an empirical assumption to soil moisture depletion in the upper soil levels (Janis, 2002). The index was developed to function throughout a wide range of climatic and rainfall conditions in forested or wild land areas. The KBDI is widely used in the Australian states of Victoria, New South Wales and Queensland operationally for fire danger ratings (Finkele *et al.*, 2006). A sample plot of KBDI generated for the whole of Australia on 22nd of September 2014 using the Australian Water Availability Project (AWAP) rainfall and daily maximum temperature data at 0.05° x 0.05° resolution is shown in Fig. 1. The underlying assumptions of KBDI are (i) rate of moisture loss due to evapotranspiration is a function of vegetation cover density, which itself is an exponential function of mean annual rainfall (ii) the evapotranspiration rate is also assumed to be an exponential function of the daily maximum temperature, and (iii) the depth of the soil layer is such that the maximum water available for evapotranspiration is 203.2 mm (8 inches). The daily KBDI filed is estimated as:

$$KBDI_t = KBDI_{t-1} - P_{Net} + ET \quad (1)$$

where KBDI is the Keetch–Byram drought index value at that location, subscripts t and $t-1$ depicts current day and previous day respectively, P_{Net} is the net accumulated rainfall valid at 9 am (local time) of the current day and ET is the daily evapotranspiration.

The net rainfall is calculated by subtracting the interception/runoff value from the accumulated rainfall amount, if the 24-hour accumulated rainfall amount or the accumulated rainfall amount over consecutive rainy days exceeds 5.08 mm. A consecutive rainfall period ends on the first day where there is no measurable rain (Rain

= 0). Thus, accounting for the net accumulated rainfall enables KBDI to satisfy the concept of consecutive and continuous water deficiency for drought indices (Byun and Wilhite, 1999).

The ET term in equation (1) is given by:

$$ET = \frac{(203.2 - KBDI_{t-1})(0.968e^{0.0875T_{Max} + 1.5552} - 8.3)}{1 + 10.88e^{-0.00173R_{annual}}} \quad (2)$$

where T_{Max} is the previous day's maximum temperature and R_{annual} is the mean annual rainfall.

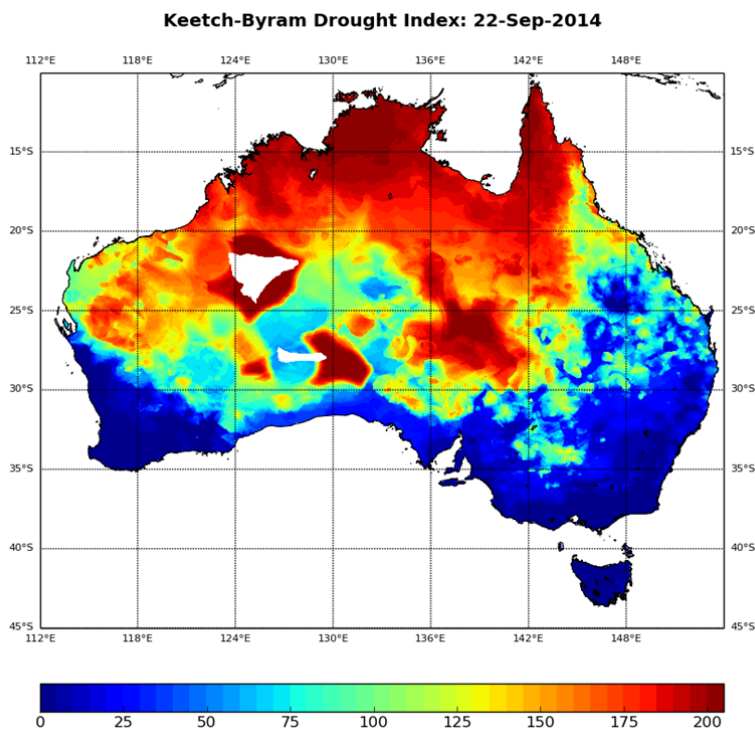


Fig. 1 KBDI for 22nd September 2014 generated at 0.05° resolution using the gridded AWAP rainfall and temperature data.

3.2 Mount's Soil Dryness Index (SDI)

SDI is the second type of soil water balance model used in Australia for drought factor calculations (Fig. 2). It was developed by Mount (1972) for Tasmanian Fire Service and are widely used in the states of Tasmania and South Australia. SDI is also used in the state of Western Australia to estimate the conditions for prescribed burning. Like KBDI, SDI also defines the soil moisture deficit, but the interception and runoff are treated separately in this case. SDI is expressed as:

$$SDI_t = SDI_{t-1} - P_{Net} + ET \quad (3)$$

where subscripts t and $t-1$ depicts current day and previous day respectively, P_{Net} is the net accumulated rainfall valid at 9 am of current day and ET is daily evapotranspiration.

$$P_{Net} = Rain - Interception - Runoff \quad (4)$$

The interception and runoff formulated in SDI is based on seven vegetation categories defined at each point of calculation. The vegetation class O represents lakes, rock and bare soil. The vegetation classes A-F depend on the vegetation type (eucalypt or pine), understorey density and tree canopy. For each category, Mount (1972) has defined values (Table 1) for canopy rainfall interception fraction (R), canopy storage capacity (C), canopy loss per wet day (W), and flash-runoff fraction (FR).

Table 1 Vegetation classes and corresponding parameter values from Mount (1972).

Vegetation Class	O	A	B	C	D	E	F
Canopy rainfall interception fraction (R)	0	0.1	0.2	0.3	0.4	0.5	0.6
Canopy storage capacity (C)	0	0.5	1.0	2.0	2.5	3.5	4.0
Canopy loss per wet day (W)	0	0.5	0.5	0.5	0.5	0.5	1.0
Flash runoff fraction (FR)	1/10	1/20	1/30	1/40	1/50	1/60	1/70

Interception is given by:

$$Interception = \begin{cases} R * Rain, & R * Rain - CW_{t-1} \leq C \\ C - CW_{t-1}, & R * Rain + CW_{t-1} > C \end{cases} \quad (5)$$

where R, and C are in Table 1.

The interception loss depends on the previous day's canopy water storage (CW_{t-1}), canopy storage capacity, and canopy rainfall interception fraction. The canopy water storage is determined by the balance between canopy rainfall interception and wet canopy evaporation loss on consecutive wet days (W, from Table 1). The canopy is assumed to dry out completely in a single dry day which follow the consecutive wet days.

$$CW_t = \begin{cases} CW_{t-1} + Interception - W, & \text{if } Rain > 0 \\ 0, & \text{if } Rain = 0 \end{cases} \quad (6)$$

Flash runoff is defined as a fraction of rainfall, and the fraction depends on the vegetation category defined by Mount (Table 1). i.e.,

$$Runoff = FR \times Rain \quad (7)$$

The ET in SDI assumes as a linear relationship with daily maximum temperature and is given by:

$$ET = a_i T_{Max} + b_i \quad (8)$$

The regression coefficients a_i and b_i are derived from the relationship between mean monthly pan evaporation and mean monthly daily maximum temperature data available from the Bureau of Meteorology's Australian Integrated Forecaster Workstation (AIFS) for state capital cities.

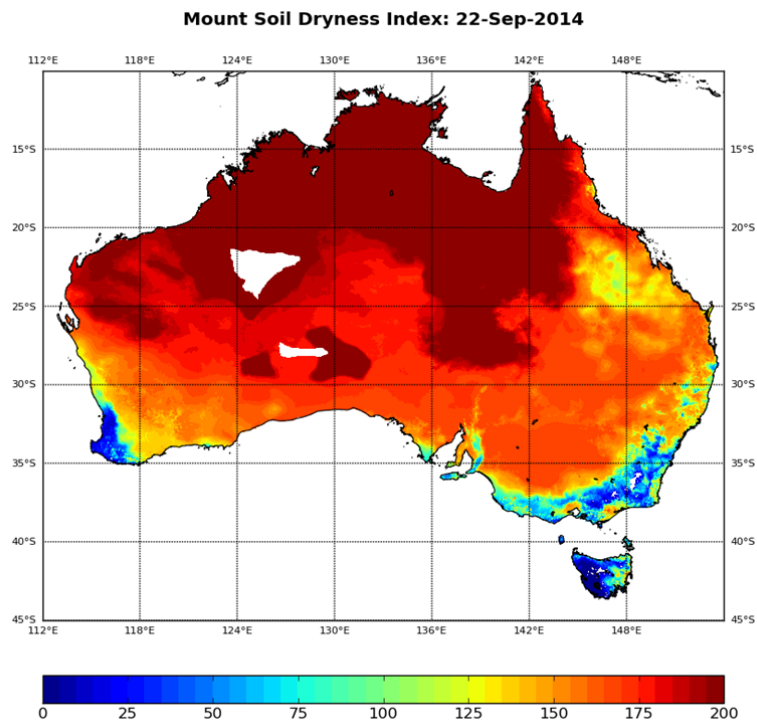


Fig. 2 Same as Fig. 1, but for SDI.

Comparisons between the KBDI and SDI made by Finkele *et al.* (2006) showed that the main difference between the two schemes is in the representation of evapotranspiration rather than the infiltration/runoff process. It was observed that SDI tend to give higher soil moisture deficits in almost all locations of Australia. This is especially noticeable in the warmer inland locations with sparse vegetation cover. The evapotranspiration in SDI is a linear function of maximum temperature and consequently follows the maximum temperature patterns, which is higher for inlands. Hence, Finkele *et al.* (2006) concluded that the use of SDI may not be appropriate at warm inland locations

of Australia. They argued that SDI is however suitable in predicting soil moisture deficits at cooler climatic zones, like the south eastern parts of Australia; where differences between SDI and KBDI are minimum as shown by both temporal averages and means over different drought factor classes.

3.3 Other indices in use internationally

Most of the FDRS used in different countries take the relationship between live vegetation moisture content and soil moisture into account by employing methods which directly or indirectly relate the fire danger index with soil moisture content. For example, the National Fire Danger Rating System (NFDRS) employed in the United States uses KBDI to estimate the proportion of live and dead fuels during prolonged drought periods (Burgan, 1988).

The Canadian Fire Weather Index (FWI) system (van Wagner, 1987; Dowdy *et al.*, 2010) includes three moisture codes that estimate the relative moisture content of three fuel layers and are calculated based on past and present weather observations of rainfall, relative humidity, temperature, and wind speed. The Fine Fuel Moisture Code (FFMC) represents the top 1–2 cm of the forest floor and numerically rates moisture content of litter and other cured fine fuels such as mosses, needles, and twigs. The Duff Moisture Code (DMC) represents the moisture content of loosely-compacted organic layers of moderate depth (5 – 10 cm). The fuels at this depth are assumed to be affected only by rain, temperature and relative humidity and not wind speed. It is also assumed that only a 24-hour accumulated rainfall amount of 1.5 mm or more has an effect on the DMC and anything below this value is intercepted by the forest canopy and fine fuel layer. The DMC fuels have a slower drying rate than the FFMC fuels and hence a seasonal day-length factor has been incorporated to account for the length of daily drying time into the drying phase of the DMC. The third and final moisture code is called the Drought Code (DC) and it is an indicator of moisture content in deep compact organic layers situated at approximately 10 – 20 cm) deep. It is assumed that only temperature and rainfall affect DC, and not the wind speed and relative humidity because of the deep location of the fuel layer. The moisture content of this layer is affected only when the 24-hour rainfall exceeds 2.8 mm, and lesser rainfalls are assumed to be lost due to interception by upper fuel layers and the forest canopy. The DC fuels also have a very slow drying rate, with a time-lag of 52 days, which is addressed by incorporating a seasonal day length factor in the drying phase. The FWI is the most widely used FDRS in the world and has been adapted by many countries including New Zealand, Mexico,

Indonesia, and Malaysia, Fiji, parts of the United States, Argentina, Spain and Portugal (Field *et al.*, 2014).

There are also many meteorologically based indices used in various European countries like France, Italy, Finland, and Sweden which relate soil moisture deficit to fire danger. All these models, like KBDI or SDI, are rather simplistic models which are empirically derived and calibrated for respective regions. The Finnish forest fire index (Heikinheimo *et al.*, 1998) describes essentially the moisture content of a soil surface layer, by estimating the volumetric soil moisture of a 60 mm thick layer using actual evaporation and precipitation data. The change in moisture state of the surface layer is essentially defined as a balance between precipitation amount after runoff and actual evaporation. The amount of rainfall runoff depends on the intensity of precipitation, with a higher intensity implying larger runoff. Actual evaporation is defined as a function of potential evapotranspiration and drying efficiency, which is empirically related to the initial or previous volumetric moisture of the surface layer. The input data for the calculation of the index comes from routine weather observations.

The French fire danger index (Willis *et al.*, 2001) combines the effects of a ‘drought index’ with wind speed as a measure of fire danger. The drought index is a measure of fuel dryness, calculated by estimating the change in soil moisture capacity which in turn depends on the daily potential evapotranspiration. Potential evapotranspiration is calculated using a formula that includes daily rainfall, temperature and relative humidity. The drought index thus provides a measure of ignition probability in addition to fuel availability. By combining drought index with wind speed, the French fire danger index accounts for the potential rate of fire spread.

The Italian Method (Dimitrakopoulos *et al.*, 2011) estimates the loss of soil moisture due to actual evapotranspiration and compares it with the potential evapotranspiration in order to compute the fire danger index. The method make use of daily average values of air temperature, relative humidity, wind speed, insolation, and cumulative precipitation.

The Swedish Meteorological and Hydrological Institute (SMHI) calculates the soil moisture values for the estimation of forest fire danger (Gardelin, 1996) using the Hydrologiska Byråns Vattenavdelning (HBV) model (Bergström, 1976; Lindström *et al.*, 1997). The HBV model relates forest fire danger to the calculated soil moisture content of an upper soil layer which has an assumed storage capacity of about 25 mm. The HBV model is basically a rainfall-runoff model, which includes conceptual numerical descriptions of hydrological processes at the catchment scale. The model is

normally run on daily values of rainfall and air temperature, and daily or monthly estimates of potential evaporation. If no evapotranspiration data is present, the values can be calculated directly from temperature data. The major land-use classes in the model are open areas, forests, lakes and glaciers. The soil moisture accounting of the HBV model is based on a modification of the bucket theory and assumes a statistical distribution of storage capacities in a basin.

4. *IN SITU* SOIL MOISTURE OBSERVATIONS

In situ soil moisture measurement techniques enable the collection of data with high precision, provided that the instruments are well calibrated. The probing depth of these ground based instruments are higher (usually 1 to 2 m to represent the vegetation root zone) compared to the remote sensing based ones (a few centimetres) which could be more valuable in a hydrologist's perspective. A number of techniques are available for ground based soil moisture measurements which are either classified as direct or indirect methods; based on whether the technique requires a contact with soil for measurements (Robinson *et al.*, 2008). Some examples of direct method include gravimetric methods (Robock *et al.*, 2000) time domain reflectometry (Robinson *et al.*, 2003), neutron probes (Vachaud *et al.*, 1977), capacitance sensors (Bogena *et al.*, 2007), cosmic-ray neutrons method (Desilets *et al.*, 2010), electrical resistivity measurements (Samouelian *et al.*, 2005), heat pulse sensors (Valente *et al.*, 2006), and fibre optic sensors (Robinson *et al.*, 2008). The indirect measurements include ground penetrating radar (Lambot *et al.*, 2006) and electromagnetic induction (Corwin and Lesch, 2005), and ground-based gravity method (Smith, 2014). A comprehensive review on each of these measurement techniques is given by Robinson *et al.* (2008), and Vreecken *et al.* (2008).

The accuracy of generally used and cost effective *in situ* soil moisture sensors like the electromagnetic sensors is affected by some inherent issues associated with calibration functions and site characteristics (Mittlebach *et al.*, 2012). Time domain reflectometry (TDR) sensors can measure the data at a higher quality than the electromagnetic sensors, but are often associated with higher costs. Further, TDR sensors have higher power consumption which could limit their use for continuous automated monitoring for a prolonged periods on specific sites that has to be operated with a stand-alone power supply.

However, the main limitation of ground based soil moisture observation techniques is that the effective area represented by these measurements are rather limited and are

about three to six orders of magnitude less than that provided by remote sensing platforms (Western *et al.*, 2002). Since soil moisture exhibits high spatial variability, this will lead to large errors of representativity (Famiglietti *et al.*, 2008); and in order to map extended spatial scales (example, continental scale), a large array of sensors are required. This could be very expensive to operate and maintain, which explains why there are very few such networks available. Despite its limited application for studying spatial variability of soil moisture, the point observations are still very useful, due to its high accuracy (provided that sites and calibration functions are properly chosen), for remote sensing and land surface and hydrological model data calibration/validation (Chen *et al.*, 2013; Paulik *et al.*, 2014).

Recently, an effort is put in place to create a data base of long-term *in situ* soil moisture measurements taken from either operational networks or validation campaigns around the globe. This collaboration called “The International Soil Moisture Network” (ISMN; Dorigo *et al.*, 2011) collects, harmonize and store the observations in a centralized data bank. The aim of ISMN is to make available an accessible global dataset for validating and improving global satellite observations and land surface models using observations taken at sites across the world which are unique in terms of climate, topography, land-use type and soil characteristics. This data set includes observations from the OzNet hydrological monitoring network managed together by Monash University and The University of Melbourne, Australia.

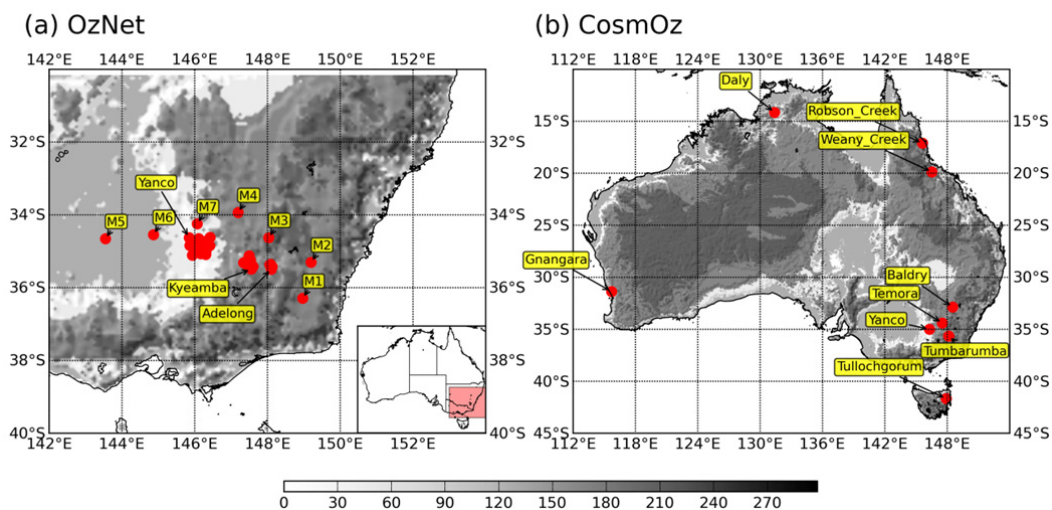


Fig. 3 Site locations of (a) OzNet and (b) CosmOz network. Spatial extent of (a) corresponds to the shaded area in its inset. The filled contours represent surface elevation (m) at 10 km resolution.

4.1 OzNet

The two main campaigns whose observations are included in this dataset are the Goulburn River campaign (Rüdiger *et al.*, 2007) and the Murrumbidgee Soil Moisture Monitoring Network (Fig. 3a; Smith *et al.*, 2012). The Goulburn dataset span for a time period of 5 years (2002 – 2007) over a catchment area of 6540 km² in the state of New South Wales. The region generally experiences a subhumid or temperate climate, with the catchment itself is subjected to high variability in rainfall and evaporation during the year. The Murrumbidgee dataset primarily constitutes soil moisture observations in vegetation root zone measured continuously at about 38 sites situated in a semi-arid to humid climate over an area of 82,000 km². The data are available from both ISMN and OzNet websites for the past ten years and is an ongoing data set (although data after May 2011 is currently embargoed).

4.2 CosmOz

CosmOz is a network of cosmic ray soil moisture probes established at thirteen locations around Australia (Hawdon *et al.*, 2014). A cosmic-ray probe measures the number of fast neutrons near the land surface. Fast neutrons are created by high-energy cosmic-ray particles interacting with atmospheric nuclei. (Desilets and Zreda, 2013). Fast neutrons are strongly moderated by the presence of hydrogen and soil moisture represents the largest and most variable source of hydrogen near the surface. Therefore, measured intensities reflect variations in the surface soil moisture. The effective depth of measurement depends strongly on soil moisture itself (Zreda *et al.*, 2008). The measurement depth decreases non-linearly with increasing soil moisture and, theoretically, ranges from about 70 cm in very dry soils to about 10 cm in saturated soils. One major advantage of cosmic-ray probes over traditional point measurement sensors is that cosmic-ray probes have a much larger horizontal footprint of about 660 m in diameter at sea level (Desilets and Zreda, 2013). The cosmic-ray probes can estimate surface soil moisture with an accuracy of about 0.02 m³/m³ (Franz *et al.*, 2012).

All the sensors in the CosmOz network are stationary and are installed above the land surface at a height of 1–2 m. CosmOz observations are obtained from the online portal <http://cosmoz.csiro.au/> managed by Commonwealth Scientific and Industrial Research Organization (CSIRO) of Australia. The data processing and calibration methods used by the CosmOz network are described by Hawdon *et al.* (2014). The locations of the CosmOz probes, used in this study, are shown in Fig. 3b.

5. REMOTE SENSING OF SOIL MOISTURE

In situ soil moisture measurements, though highly reliable, could be cost-prohibitive for extended spatial mapping. Since soil moisture exhibits spatial variability depending on the topography of an area and the soil characteristics, methods to characterize it on a regional scale without the necessity for exhaustive manual measurements would be beneficial for applications like fire and flood forecasting. Remote sensing using aircrafts or satellites offers the potential for large spatial coverage (even global in case of satellites) of high-resolution, aggregated soil moisture mapping (Lakshmi, 2013). Advances has been made in active and passive satellite remote sensing techniques to provide unique capability of measuring soil moisture at regional and global scale which satisfy the science and application needs of hydrology. The theory of soil moisture remote sensing stems from the fact that the electromagnetic response of land surface is modified by its soil moisture content (refer Appendix A for basic theory). Various regions of the electromagnetic spectrum have been used to estimate soil moisture, including gamma radiation (Carroll, 1981), thermal infrared (Price, 1982), and passive and active microwave (Jackson *et al.*, 1996). There are many factors that modulate the radiation reaching the sensor; for example surface temperature, surface roughness, vegetation, atmospheric effects etc. However, these effects are negligible at low frequencies of microwave spectrum (roughly 1 – 5 GHz), making them an appropriate spectral range for soil moisture measurements. Further, longer wavelengths have a higher capacity to measure deeper (2 – 5 cm) soil moisture layers, the penetration depth being of the order of one tenth of the wavelength (Lakshmi, 2013). These are significant advantages of microwave remote sensing and hence there has been considerable amount of research done to determine soil moisture in low-frequency microwave spectra (Jackson and Schmugge, 1995; Jackson *et al.*, 1999).

The earliest efforts to determine soil moisture from space-borne microwave sensors for large spatial scale hydrological studies started with the availability of Scanning Multi-channel Microwave Radiometer (SMMR; Njoku *et al.*, 1998) and Special Sensor Microwave Imager (SSM/I; Hollinger *et al.*, 1990) data sets. Investigators used data from these two instruments for soil moisture retrievals, sensitivity and scaling studies at different spatial scales and also in conjugated studies with land surface models (Paloscia *et al.*, 2001; Guha and Lakshmi, 2002; Wen *et al.*, 2005; Lakshmi *et al.*, 1998). Figure 4 depicts a schematic overview of the past, present and future soil moisture remote sensing missions. The following sub-sections describe the available historical and current space-borne data sets.

5.1 SMMR

The historic data set from SMMR spans from 1978 – 1987 and is based on C-band (6.63 GHz) passive microwave measurements. The effective sensing depth of C-band data is roughly 1 cm. The SMMR data were found to be more relevant in regions of transition from wet to dry climate, because the data was affected by dense vegetation over wet regions and the high level of noise in the data masked the small variability in dry regions. Validations against ground based observations showed that the SMMR dataset exhibits a large bias of about $0.1 \text{ m}^3/\text{m}^3$ in volumetric soil moisture content (Reichle *et al.*, 2004).

5.2 SSM/I

The SSM/I data set is available since 1987 and uses the 19.4 GHz Ku-band channel measurements to retrieve soil moisture information. A recent study by van der Velde *et al.* (2014) using a new retrieval algorithm achieved a root mean square error of $0.046 \text{ m}^3/\text{m}^3$ over Tibetan Plateau, which is almost in agreement with the accuracy requirements of satellite missions specifically dedicated to soil moisture. However, different studies on SSM/I observations has concluded that even though soil moisture retrieval is possible using the SSM/I dataset, the accuracy is limited for dense vegetation and cloud conditions (Wen *et al.*, 2005; Jackson *et al.*, 2002). This is somewhat the characteristics of most frequencies in the higher end of the soil moisture sensitive spectra where scattering by vegetation canopies competes with soil moisture in governing the spectral gradient.

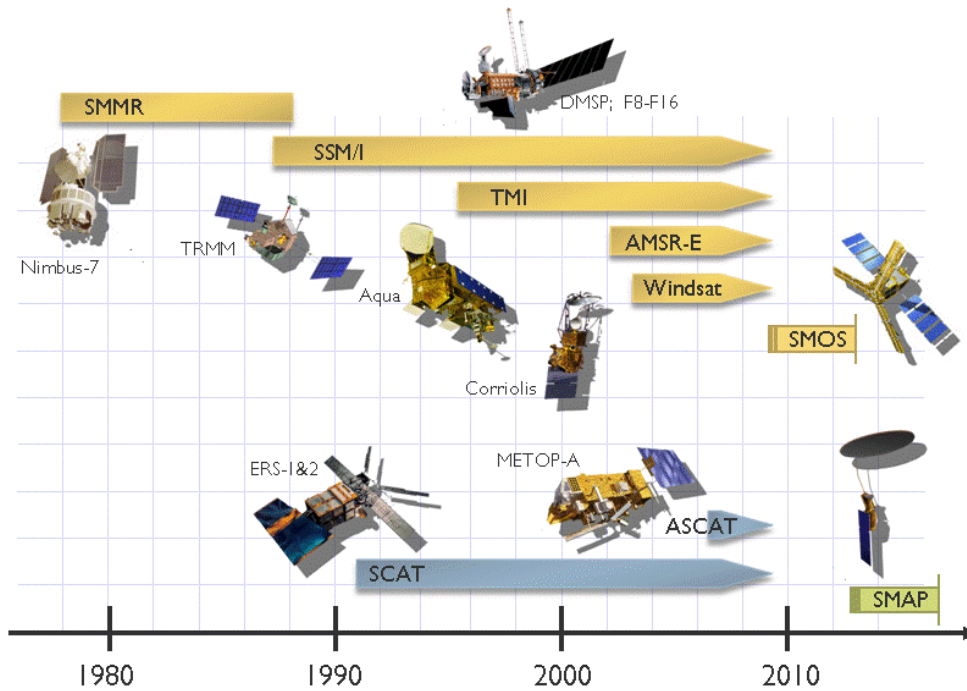


Fig. 4 Overview of soil moisture remote sensing from space – missions and their timelines. Courtesy: European Space Agency and Technische Universität Wien.

5.3 WindSat

WindSat passive microwave data at 10, 18.7, and 37 GHz were used to produce global retrievals of soil moisture and were then validated against climatologies and in situ network data (Li *et al.*, 2007). The authors found that the retrieved volumetric soil moisture values were in good agreement with the truth and the mean bias observed was about $0.004 \text{ m}^3/\text{m}^3$, which was within the requirements for most science and operational applications. The retrieved SM distributions are also found to be very consistent with global climatology and mesoscale precipitation patterns.

5.4 TRMM

Successful soil moisture retrievals were also carried out from Tropical Rainfall Measuring Mission (TRMM) Microwave Imager (TMI; Gao *et al.*, 2006). The TRMM data set is available from 1997 and are based on X-band (10.65 GHz) passive microwave observations. Like C-band, the effective sensing depth of X-band is also restricted to first 1 cm of soil layer. Gao *et al.*, 2006 compared the TMI soil moisture estimates against the Oklahoma Mesonet observations for a period of four years, and

found that that the retrieved product is comparable to the in situ soil moisture values, with an average seasonal correlation of 0.59. Further, the TMI soil moisture product exhibited a consistency with the corresponding precipitation field.

Table 2 Validation studies of sensors against the *in situ* observations.

Instrument	Resolution	Study Area	Literature Source	Validation Metric		
				Bias (m^3/m^3)	RMSD (m^3/m^3)	Correlation
SMMR	~25 km	Global	Reichle <i>et al.</i> , 2004	0.01	—	0.45
SSM/I	~25 km	Tibet	van der Velde <i>et al.</i> , 2014	—	0.046	—
ERS	50 km	Sahel	Gruhler <i>et al.</i> , 2010	0.042	0.054	0.52
AMSR-E*	60 km	Australia	Draper <i>et al.</i> , 2009	—	0.013 to 0.066	0.54 to 0.94
AMSR-E#				-0.01 to 0.19	0.05 to 0.19	0.45 to 0.92
ASCAT ⁺	35 km	Australia	Abergel <i>et al.</i> , 2012	-0.021	0.184	0.80
SMOS ⁺	40 km	Australia	Abergel <i>et al.</i> , 2012	0.195	0.255	0.74
AMSR2 ⁺	60 km	Australia	Rudiger <i>et al.</i> , 2013	-0.01 to 0.05	0.04 to 0.09	—

Note that studies with only one value for each metrics implies the mean values and with a range implies that deduces from each sites over the catchment/basin. (*) validation against filtered and bias corrected AMSR-E dataset; (#) validation against the original AMSR-E dataset. (+) To enable a fair comparison, both *in situ* and remotely sensed soil moisture data sets are scaled between [0,1] using their own maximum and minimum values.

5.5 ERS

ERS Scatterometer which is a vertically polarized radar operating at C-band (5.3 GHz) is another historical data set available for soil moisture studies. It has been flown on board of the European Remote Sensing Satellites (ERS) –1 (1991 – 1996) and –2 (1995 – 2011). The instrument measures the backscattering coefficient from three different antennas with one looking normal to the satellite track, another one pointing 45° forward, the third one pointing 45° backward with respect to the satellite flight track. The spatial resolution is about 50 km with a swath width of 500 km. A soil moisture index, which is representative of surface (0 – 5 cm) soil moisture at watershed scale, can be derived from ERS-Synthetic Aperture Radar (ERS-SAR) data (Quesney *et al.*, 2000). Wagner *et al.* (2007) through statistical analysis on ERS-SAR datasets found out that these retrieved soil moisture products contribute effectively to the monitoring of trends in surface soil-moisture conditions, but not to the estimation of absolute soil-moisture values. An independent validation study by Drusch *et al.* (2004) found that, when validated against the Southern Great Plains field experiment, the ERS scatterometer datasets (both ERS–1 & –2) show a reasonably good temporal evolution of soil moisture and the root mean square errors were at 0.057 m³/m³. The authors also compared the ERS derived surface soil moisture product against the ERA reanalysis and found a high correlation between them, indicating that the retrievals are as accurate as the reanalysis data set. The ERS soil moisture product has also been validated against *in situ* observations located at three representative sites along a North-South climatic gradient in the African Sahel region (Gruhler *et al.*, 2010). The authors generally obtained good consistency between the ERS satellite soil moisture product derived using the TU Wien algorithm remapped at 12.5 km grid resolution and ground observations, with consistent spatial distribution compared to the other sensors assessed. The correlation, RMSE error and bias obtained over the Sahel region was 0.52, 0.054 and 0.042 respectively. The ERS is succeeded by the MetOp mission which is described in a following paragraph.

5.6 AMSR-E

Another data available is from the Advanced Microwave Scanning Radiometer – Earth Observing System (AMSR-E; Njoku, 2006) on NASA’s Aqua satellite and which is developed by National Aeronautics and Space Administration (NASA) in collaboration with the Vrije Universiteit Amsterdam (Owe *et al.*, 2008). Soil moisture retrievals are produced from the C-band (6.92 GHz) passive brightness temperature observations and a Land Parameter Retrieval Model (LPRM). Due to radio frequency interference (RFI)

in the C-band over north America, NASA also produced a soil moisture product from X-band (10.65 GHz) using a different algorithm (Draper *et al.*, 2009). These products have been extensively validated against field observations over different regions (Wagner *et al.*, 2007; Draper *et al.*, 2009; Brocca *et al.*, 2011) and are found to be of good agreement. For example Draper *et al.*, 2009 validated the AMSR-E data, generated using the Vrije Universiteit Amsterdam – NASA algorithm and which contains soil moisture retrievals from both the C- and X-band, with the in situ observations from the Murrumbidgee and Goulburn field campaigns in south-eastern Australia and found that for a normalized and filtered data the correlations and root mean square errors were 0.8 and 0.03 m³/m³ respectively. However, the validations with original data yielded a much higher errors (Table 1) which in some cases were three times that from the normalized and filtered one. They argued that filtering and normalization is essential for effective scaling and comparison with ground observations as the data is prone to high level of noise, bias and variability. However, it is worth noting that the filtered and normalized data tend to miss the sudden increase in soil moisture content due to large precipitation event, a feature aggravated by the filtering they did on AMSR-E data in the form of five day moving average. The AMSR-E data set spans from 2002 – 2013, and ceased operations in October 2013 due to a mechanical failure of the spinning mechanism. It is not clear at the moment whether the operations would be restarted for AMSR-E.

5.7 SMOS & ASCAT

There are currently two operational missions for soil moisture observations as part of European Space Agency's "Living Planet" programme; the Microwave Imaging Radiometer with Aperture Synthesis (MIRAS) on board Soil Moisture and Ocean Salinity (SMOS) satellite, and the Advanced Scatterometer (ASCAT) on board meteorological satellites MetOp-A/B. The ASCAT data from MetOp-A is operationally received in the Australian Bureau of Meteorology. Figure 5 shows a typical time averaged soil moisture products retrieved in early October from ASCAT and SMOS missions over Australia. The SMOS satellite was launched successfully in November 2, 2009 with data available from November 20, 2009. MIRAS on board the SMOS mission operates at L-band (1.4 – 1.427 GHz) frequencies and provide global maps of soil moisture and vegetation water content with an accuracy of about 0.04 m³/m³ and 0.5 kg/m² respectively at a pixel resolution of 35 km at nadir to ~90 km at the scan edges (Kerr *et al.*, 2001). In order to achieve the higher spatial resolution required for soil moisture measurements in L-band without the need for a huge antenna, the aperture

synthesis technique was employed, where the large antenna size required has been simulated through 69 small antennas distributed over the three arms and central hub of the MIRAS instrument. An exhaustive validation study conducted by Albergel *et al.* (2012) on SMOS and ASCAT datasets using *in situ* observations located around the world found a satisfactory mean correlation of 0.54 and 0.53 respectively. On the disaggregation of analysis over different regions, they obtained a correlation of 0.74 for SMOS and 0.80 for ASCAT over Australia, which is one of the highest among all the regions. They attribute this higher correlations observed over Australia to two reasons; (i) Australia is minimally affected by the Radio Frequency Interference (RFI) effects which disturbs the natural microwave emissions and, (ii) OzNet sites are predominantly located over regions of significant bare soil fraction and/or dry vegetation caused by the crop rotation practice. Another study by Sánchez *et al.* (2012) during a period from January to December in 2010 using 20 *in situ* soil moisture stations from the REMEDHUS network in Spain found an acceptable level of agreement between the *in situ* and satellite data with a correlation of 0.73, root mean square error $0.069 \text{ m}^3/\text{m}^3$, bias of $0.053 \text{ m}^3/\text{m}^3$ and a centred (bias removed) root-mean-square difference of $0.044 \text{ m}^3/\text{m}^3$. However, other validation studies done at locations in United States (Al Bitar *et al.*, 2012) and Europe (Lacava *et al.*, 2012; Dall'Amico *et al.*, 2012) found a slight under-estimation in the SMOS soil moisture. On a positive note, it is worth noting that the results from all these studies concluded that the SMOS could successfully achieve the accuracy objective of $0.04 \text{ m}^3/\text{m}^3$ at most of the validation sites.

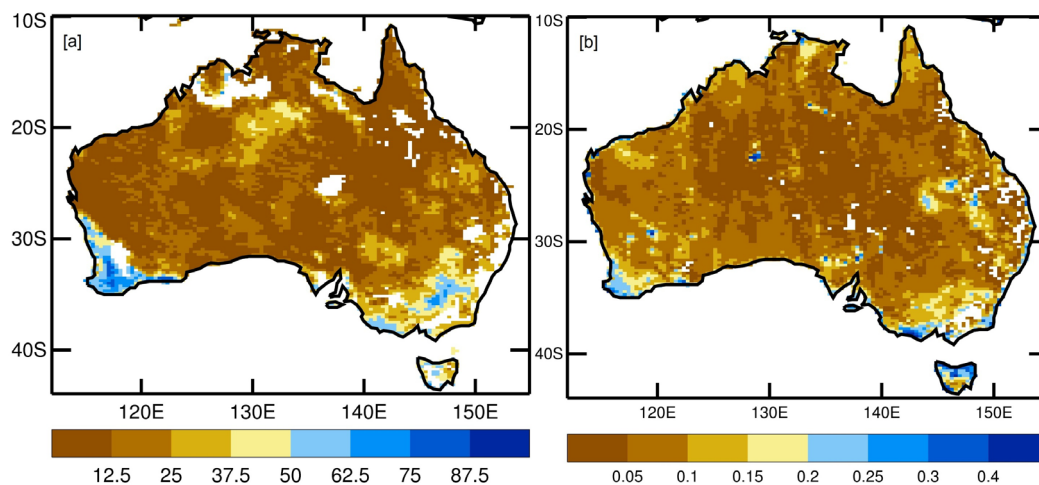


Fig. 5 Three-day (4 – 6 October 2014) averaged maps of retrieved (a) soil wetness index from ASCAT and (b) volumetric soil moisture content from SMOS satellite over Australia.

5.8 AMSR2

The Global Change Observation Mission-Water (GCOM-W; Imaoka *et al.*, 2010) launched by the Japanese Space Agency is another instrument which provides microwave observations of land surface. GCOM-W1 was launched successfully on May 17, 2012 and began collecting data on July 4, 2012. The Advanced Microwave Scanning Radiometer-2 (AMSR2) is the sole instrument on board the GCOM-W1 mission and is a successor of the AMSR-E instrument on board EOS-Aqua satellite with some improvements in the calibration system and an addition of 7.3 GHz channel to mitigate the radio-frequency interference issue seen in AMSR-E. An initial evaluation of the Level 3 soil moisture products from AMSR2 using *in situ* hydrological observation data from the OzNet monitoring network across south-eastern Australia showed that the root mean square error is about 0.04 – 0.09 m³/m³ (Rüdiger *et al.*, 2013). An extensive monitoring and validation campaign of AMSR2 on board GCOM-W1 is undertaken in the Australia Murray Darling basin (Walker *et al.*, 2012) and are expected to see more outcomes from the project in the near future.

5.9 Recent / future platforms

The space-borne observational network of soil moisture is anticipated to grow further with several launches planned in near future. An example of a state-of-art platform which was launched recently (on 31st January 2015) is the Soil Moisture Active/Passive mission (SMAP) by NASA. SMAP is an advanced system which consists of both passive and active microwave sensors and is expected to provide soil moisture measurements at a much higher resolution than the current passive radiometers. SMAP is designed to provide for data disaggregation, where the high resolution (~1 km) radar data is used to disaggregate coarser resolution (~36 km at nadir) passive radiometer data (Lakshmi, 2013). MetOp-C which will carry another ASCAT instrument is expected to be launched in 2016 and will provide supplement the already existing MetOp-A/B ASCAT observations. The Argentine Space Agency is planning the launch of two Microwaves Observation Satellites SAOCOM-1A and SAOCOM-1B in 2014/15, both of which will be equipped with a L-band (1.275 GHz) full polarimetric Synthetic Aperture Radar. Thus the addition of all these planned satellites is expected to provide an uninterrupted stream of daily soil moisture observations well beyond 2020.

Different studies of sensor and retrieving algorithm validation have used diverse methodologies and reference datasets (both in location and instrumentation) for their purpose, making it very difficult to assess the relative accuracy of these sensors and

their respective algorithms to retrieve soil moisture. This is even true for the same sensors studied and validated across different climate regimes and vegetation zones. Nevertheless, we try to summarize the results from the studies made on each sensor and mentioned in the above paragraphs as a table (Table 1) for the interest of readers.

The results from the above mentioned validation studies show that soil moisture products from satellite sensors are of high quality and generally capture the temporal variability of soil moisture to a good extent. For sensors like AMSR-E, ASCAT and SMOS, which has been validated in contrasting biome and climatic conditions, the temporal correlations with *in situ* data look rather satisfactory. A lot of research is undertaken to improve the retrieval algorithms used to derive the soil moisture products from existing platforms (Nichols *et al.*, 2001). Such improved products have shown higher accuracy (Velde *et al.*, 2014; Draper *et al.*, 2009) compared to the older ones. With the sensors and their retrieval algorithms continue to improve, the confidence in soil moisture products from remote sensing is expected to only increase.

6. LANDSCAPE WATER BALANCE MODELS

Landscape water balance models allow to assess water resources and their availability for use at a regional and continental scale. They provide information on water distribution, storage, availability, and use by taking into account the local climatic and hydrological conditions. Two prominent landscape water balances model used in Australia are the Australian Water Resources Assessment (AWRA; van Dijk, 2010) system and the WaterDyn (Raupach *et al.*, 2009). These two models are run at daily time steps with a spatial resolution of 5 km.

The AWRA system is operational in Bureau of Meteorology and provides daily updates of catchment water balance. It constitutes of three components, (i) a landscape component which accounts for the vegetation water use and soil water dynamics (ii) a river component which describes the surface water body dynamics, open water evaporation and catchment water yield, and (iii) a groundwater component which calculate the groundwater flow estimates. AWRA system is calibrated against a range of observations including ground measurements such as river gauges, irrigation diversion metering, soil moisture sensors and satellite observations of vegetation cover, flooding, soil moisture, precipitation, evaporation and groundwater dynamics.

WaterDyn considers terrestrial water balance in the unsaturated soil column, spatially resolved across the whole Australian continent. It thus accounts for transpiration, soil

evaporation, leaching and deep drainage. The model is defined on two soil layers of depth 0.2 (surface to 0.2m deep) and 1.3 m (0.2 to 1.5 m). It has an option to include a sub-model to calculate dynamic vegetation cover fraction and leaf carbon. This model is run operationally as part of the AWAP project to monitor the state and trend of the terrestrial water balance of the Australian continent.

Evaluation of AWRA and WaterDyn against catchment observations show that AWRA performs better than WaterDyn (Frost, 2014). However, this is not surprising as AWRA is calibrated against a wide range of observations, whereas WaterDyn is not. Frost (2014) also benchmarked these two models against an uncalibrated Community Atmosphere Biosphere Land Exchange (CABLE; Kowalczyk *et al.*, 2013) land surface model. The results show that, although AWRA and WaterDyn skills in simulating evapotranspiration and root zone soil moisture are lower than that of CABLE, they perform reasonably well. Currently, these landscape water balance models are driven by observation based analyses at a daily time step. At present, these models are only used operationally for water resource assessment and doesn't provide any forecasting capability. This may limit their applicability for fire danger ratings. Further, the operational version of these models are run at a coarse temporal resolution (daily). There is a lack of literature in the suitability of AWRA and WaterDyn models at sub-daily scales and their accuracy in simulating diurnal variation of soil energy and water states. Further, the operational version of these models are yet to be incorporated with advanced data assimilation techniques to constraint the soil hydrology. It should be therefore assumed that, though there is potential, these models are rather not useful in their current form for fire prediction applications.

7. LAND SURFACE MODELS

Land surface models (LSMs) are another source which could provide good estimates of soil moisture. They represent processes which regulate the exchanges of water and energy through the soil–plant–atmosphere continuum. This is achieved through the detailed representation of the transport of momentum, heat and water in the continuum; and depiction of thermal and hydrological processes in the soil and snow (Best *et al.*, 2011). Land surface models have evolved a lot in recent years and can now account for plant physiology, vegetation dynamics, carbon assimilation and groundwater dynamics (Niu *et al.*, 2011). Most of the LSMs represents the soil moisture as a prognostic variable. The simulated soil moisture is rather a model specific quantity and may vary from model to model. Some of the prominent LSMs are Joint UK Land Environment Simulator (JULES; Best *et al.*, 2011; Fig. 6) developed in the United Kingdom, NOAA

LSM whose development is spearheaded by the National Centre for Environmental Prediction in the United States (Chen and Dudhia, 1996; Koren *et al.*, 1999) and the CABLE model (Kowalczyk *et al.*, 2013) developed in Australia.

The land surface models form an integrated part of NWP and climate models and provide lower boundary conditions to them. In Australia, for example, the operational global NWP system called Australian community Climate and Earth Simulator (ACCESS) employed by the Bureau of Meteorology incorporates the Met Office Surface Exchange Scheme version 2 (MOSES2, Essery *et al.*, 2001) LSM, which is a predecessor to JULES. The next updated version of ACCESS will use JULES, with operational testing currently under way. In MOSES2 (and generally in all LSMs), the prognostic equation for soil moisture is given by Richard's equation which is derived from Darcy's law under the assumption of a rigid, isotropic, homogeneous, and one-dimensional vertical flow domain. The MOSES2 soil is 3 m thick and is discretised into four layers of 0.1, 0.25, 0.65 and 2 m thickness from top to bottom. The simulated soil moisture from MOSES2 are given in the units of mass per unit area (kg/m^2). The climate mode of ACCESS uses the CABLE LSM, developed locally in Australia. CABLE also uses the Richards' equation for soil water estimation and has six discrete soil layers. Work is now undertaken to incorporate CABLE into the NWP system.

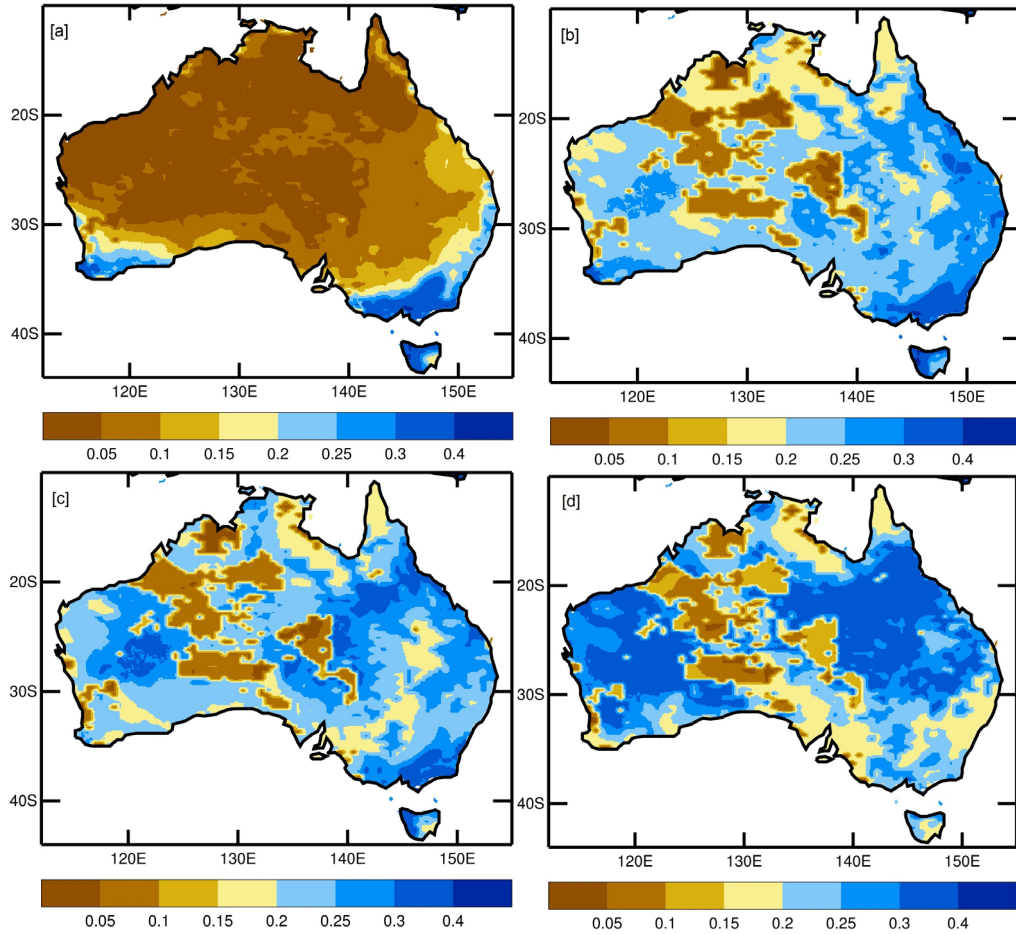


Fig. 6 Volumetric soil moisture content at layers (a) 0.0 – 0.1 m, (b) 0.1 – 0.35 m, (c) 0.35 – 1.0 m, and (d) 1.0 – 3.0 m from the JULES LSM which is coupled to the regional ACCESS numerical weather prediction model. The model resolution is 12 km x 12 km.

7.1 LSM inputs

LSMs can be run either in a coupled mode, where it is integrated with an atmospheric model, or as stand alone which can be run by offline input parameters and forcing data. In the first case the forcing data used to drive the LSM are outputs from the atmospheric model which it is coupled to. The offline version can have all forcing fields and parameters obtained from a single source or from multiple sources. The common forcing fields to drive an LSM and their SI units are given in Table 2. For offline simulations in a regional scale, gridded observational analyses are generally used to drive the LSMs. The temporal resolution of these forcing data are crucial depending upon the LSM application and is found to have an impact on model water balance

(Compton and Best, 2011). It was found that the evaporation tend to decrease with a decrease in the resolution of forcing data because of the fact that the peak in shortwave radiation are not captured well enough by the coarser dataset. This inturn produced a higher run-off, since LSMs close the water budget by construct. Compton and Best (2011) also studied the effect of forcing fields with different spatial resolution and found that due to larger peak precipitation rates in high resolution datasets, vegetation canopy interception decreases resulting in less canopy evaporation, but compensated by a larger evaporation from the soil.

High temporal resolution data for global LSM research simulations are generally achieved through the use of atmospheric reanalysis products like National Centre for Environmental Prediction–National Centre for Atmospheric Research (NCEP–NCAR; Kalnay *et al.*, 1996) reanalysis or the European Centre for Medium Range Weather Forecasts (ECMWF) Reanalyses (ERA) –40 (Uppala *et al.*, 2005) and –15 (Gibson *et al.*, 1997). A reanalysis is produced using unchanged (frozen) versions of numerical weather prediction and assimilation systems that blends in a variety of atmospheric and sea surface observations to provide optimal grids of long-term, continuous atmospheric and land surface fields in time and space. Although the reanalysis contains biases, they have the advantage of consistency needed to force LSMs for a longer period. However, these reanalyses usually have a temporal resolution of 6 hours which could be problematic for specific applications. National NWP centres also perform analyses as part of their routine operational NWP runs, where advanced data assimilation techniques are used to produce an optimal atmospheric state from observations and model forecast valid at that time. This analyses serves as the initial condition for the next set of NWP forecasts. With an increasing computational resources, these analyses could be made at a much shorter time steps (3 hours or even less) in future which could be useful in an LSM perspective. However, unlike reanalyses this NWP analyses could undergo rapid changes as the centres always explore the possibility of improvements in model resolution and physics, usage of more number and types of observations etc. Another important issue with NWP is the errors in their precipitation fields, which could adversely affect the LSMs capability to estimate the root-zone hydrologic conditions. Mitchell *et al.* (2004) demonstrated that the first-order errors in the LSM simulations were due to inaccurate specification of the forcing fields, especially the precipitation. The advantage of operational NWP analyses and forecasts however is that it presents and opportunity to run the LSMs almost real-time.

Table 3 Generic meteorological forcing variables required to drive an LSM.

No	Forcing Variable	Units
1	Downward component of shortwave radiation at the surface	W m^{-2}
2	Downward component of longwave radiation at the surface	W m^{-2}
3	Rainfall	$\text{kg m}^{-2} \text{s}^{-1}$
4	Snowfall	$\text{kg m}^{-2} \text{s}^{-1}$
5	Wind speed	m s^{-1}
6	Atmospheric temperature	K
7	Atmospheric specific humidity	kg kg^{-1}
8	Surface Pressure	Pa

A few observation based analyses are also available which could be useful for driving a LSM for applications such as fire prediction. For example, in Australia there are mainly two observations based analyses available, the Mesoscale Surface Analysis System (MSAS; Glowacki *et al.*, 2012) and the Australian Water Availability Project (AWAP; Jones *et al.*, 2009) analysis. MSAS is developed at the Australian Bureau of Meteorology and aims to create an operational gridded surface analysis which mitigate problems arising due to inhomogeneous observation distribution in space and time. MSAS gives hourly analyses of atmospheric pressure at mean sea level, potential temperature, 2-m dewpoint temperature, and 10-m wind components that are generated on a 4-km grid. The MSAS fields are found to be significantly more accurate than the current operational NWP model fields and are on par with similar analysis systems employed in different parts of the world. The AWAP dataset includes a range of improved meteorological analyses and remotely sensed datasets for Australia which include analyses of rainfall, temperature, vapour pressure and wind at daily and monthly timescales on $0.05^\circ \times 0.05^\circ$ spatial grid. The dataset is created by applying topography-resolving analysis methods to *in situ* observations of rainfall, temperature and vapour pressure to produce analyses for a period from 1900 to the present. The resulting analyses proved to be a substantial improvement on the preceding operational analyses produced by the Bureau of Meteorology and are widely used in Australia for climate studies (King *et al.*, 2012). However, it is worth noting that both MSAS and AWAP doesn't produce all the variables required (Table 2) to drive an LSM. Further, the

AWAP data are available only on a daily basis which limits its use for sub-daily land surface calculations. However, data disaggregation methods can be employed to create sub-daily fields out of the daily ones (Williams and Clark, 2014).

Inherently, due to the inadequacies of model physics, errors in representativity, parsimonious numerical representation of highly nonlinear physical processes, and limited accuracy of the input static parameters, meteorological forcing and initial conditions, the soil moisture hydrology simulations by LSMs often exhibit large uncertainties (Henderson-Sellers *et al.*, 1995; Godfrey and Stensurd, 2008). Data assimilation systems allow us to offset such uncertainties to some extent by routinely updating the hydrological conditions using information provided by observations on state variables used by LSMs (Dharssi *et al.*, 2011; Draper *et al.*, 2009). The following section gives a brief overview on the background and advances made in the field of land surface data assimilation.

Table 4 Generic ancillary data required by an LSM

Parameters	Units
Land cover	
Green vegetation fraction	
Topographical elevation	m
Soil type	
Land-sea mask	
Volumetric wilting point for soil	$\text{m}^3 \text{m}^{-3}$
Dry soil thermal capacity	$\text{J K}^{-1} \text{m}^{-3}$
Dry soil thermal conductivity	$\text{W m}^{-1} \text{K}^{-1}$
Volumetric saturation point for soil	$\text{m}^3 \text{m}^{-3}$
Critical volumetric soil moisture content of soil	$\text{m}^3 \text{m}^{-3}$
Soil Saturated hydraulic conductivity of soil	$\text{kg m}^{-2} \text{s}^{-1}$
Bare soil albedo	

7.2 Land surface data assimilation

Data assimilation is the process through which real world observations enter the model's forecast cycles, provide a safeguard against model error growth and contribute to the initial conditions for the next cycle. Large differences between model and observations may exist and hence observations are assimilated to correct each short-range forecast that serves as the basis for the next analysis, resulting in a series of small corrections to the model forecast. Ideally, the model forecast would be corrected to the "true" state of the atmosphere within the limits of what the model is able to predict based on its resolution and physics. Data assimilation involves a number of distinct steps like (i) ingesting the data, (ii) decoding coded observations (iii) weeding out bad data, (iv) comparing the data to the model's short-range "first-guess" fields, and (v) adjusting the data (in the form of model corrections) onto the model grid for making the forecast. This process thus blends information from the short-range forecast with information from the new observations.

One of the approach in land surface assimilation is to use an indirect method, where the evolving screen-level temperature and humidity — through their assimilation — are used to estimate soil temperature and moisture (Vinodkumar *et al.*, 2009). This method makes use of the denser screen level observations available, and surrogates the sparseness of hydrological observations to some extent. ACCESS NWP system employs a similar physically based soil moisture nudging technique (Best *et al.*, 2007). The nudging scheme in ACCESS is physically based as it uses the model equations and the model soil and vegetation parameters (e.g. wilting point, field capacity, fraction of bare soil, vegetation root depth). The model wilting point and field capacity parameters have a significant impact on the magnitude of the analysed soil moisture. While the fraction of bare soil and vegetation root depth parameters significantly modulate the vertical variation of the soil moisture nudges. Since errors in forecasts of screen temperature and humidity are due to many factors, the ACCESS soil moisture nudging scheme seeks to identify and correct for those errors in forecasts that are due to the model soil moisture. The ACCESS NWP soil moisture nudging scheme is only active in unstable conditions (negative Richardson number), where the errors in screen temperature and humidity are of opposite sign (i.e. model boundary layer too warm and dry or model boundary layer too cold and moist), where there is evaporation, and where there is no snow cover. The soil moisture nudging is performed four times a day and only adjusts model soil moisture for the portion of the globe in daylight. The soil moisture nudging scheme can correct the model soil moisture not only for random errors but also for persistent systematic errors in the model such as biases in the model

precipitation. A significant disadvantage of the soil moisture nudging scheme is that the model soil moisture can become updated for model errors that are unrelated to soil moisture. The soil moisture nudging scheme only uses observations of screen level temperature and humidity and doesn't use any remotely sensed observations or any observations of precipitation.

However, with the advances made in microwave remote sensing of soil state through dedicated satellites launched for hydrologic monitoring, spatially comprehensive observations can now be available at larger scales. Numerous studies have been conducted on the use of such datasets in conjunction with land data assimilation systems (e.g., Dharssi *et al.*, 2011). The availability of more and more observations, especially satellite ones, spurred significant advances to be made in land surface data assimilation in a short period of time. This was also helped by the knowledge gained from the experience of data assimilation in the field of meteorology and oceanography. Today, advanced approaches in data assimilation like the Extended Kalman Filter (Dharssi *et al.*, 2012) are widely used by land surface modelling community to get the best estimate on fields of primary interest, like the soil moisture content. The advantage of Kalman filter based data assimilation techniques is that it allows flexibility in handling all sources of uncertainties along with the possibility of ingesting the data sequentially as it becomes available. These algorithms can also make use of both screen level and remote sensing observations and are found to be superior to the earlier used techniques like optimal interpolation (de Rosnay *et al.*, 2012).

The idea that remote sensing and land surface models are somewhat complementary, as the former could give discontinuous but spatially comprehensive and relatively accurate measurements of the hydrologic system, and the later give the temporal and spatial state of the entire system variations albeit with larger errors, gives an opportunity to optimally merge these two data types to derive a best possible hydrologic system state estimation. The general outcome of the studies which ingested surface soil moisture products from various satellites is that the assimilation of this products yield a better estimate of the soil moisture.

Walker and Houser (2004) demonstrated that in order to see an improvement in the analysis of soil moisture due to assimilation of remote observations, the observation errors should be less than the model forecast errors. However, Draper *et al.* (2012) found that, even though correlation between *in situ* measurements and an open-loop (no assimilation) LSM run (R_{im}) was better than that between the *in situ* and satellite data (R_{ir}), assimilation of this satellite data still yielded positive impact on the analysed soil

moisture. Their analysis showed that assimilation of satellite observation with R_{ir} , no more than 0.2 below R_{im} , generally increased the soil moisture skill up to 40 per cent as R_{ir} increased relative to R_{im} (Fig. 7). In this context, it is also important to understand that the remotely sensed observations itself could have biases associated with it mainly due to instrument calibrations, drift due to ageing, spatial representativeness and limitations in retrieval algorithms or forward models calculations. Hence it is essential to quality control and bias correct the satellite data using different methods like cumulative distribution function (CDF) matching (Reichle and Koster, 2004; Drusch *et al.*, 2005).

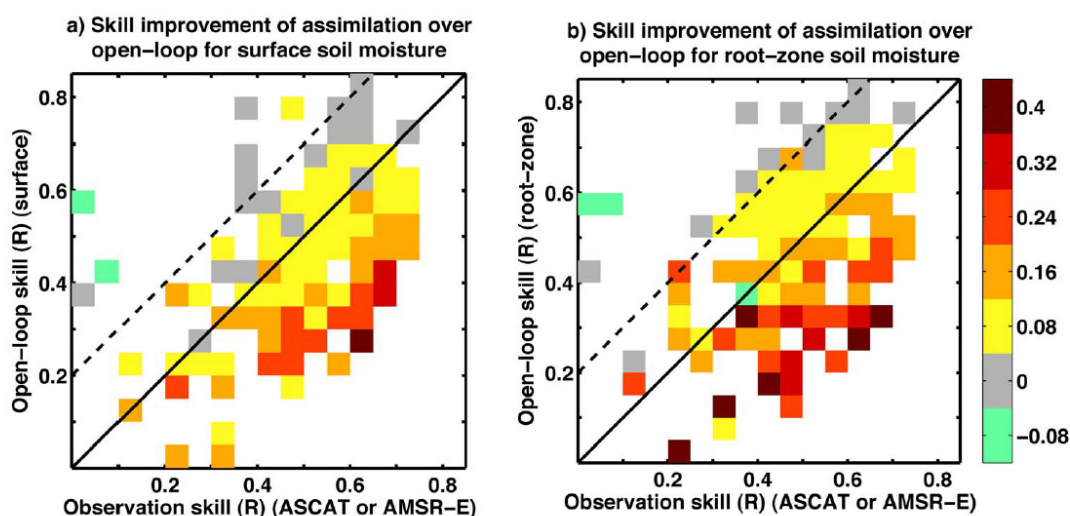


Fig. 7 Skill improvement from assimilating either ASCAT or AMSR-E for (a) surface and (b) root-zone soil moisture, as a function of the open-loop and observation skill. The results show that assimilation can improve skill, provided the observation skill minus open-loop skill > -0.2 . Skill is defined as the temporal correlation against ground based observations. Courtesy: Draper *et al.* (2012).

8. CONCLUSIONS

Knowledge of soil dryness is critical for the management of bushfires and contribute significantly to the release of early fire warnings. The McArthur's Forest Fire Danger Rating System currently employed in Australia uses very simple empirical based sub-models called KBDI or SDI to calculate the moisture depletion in the upper soil layers. This methods were developed in 1960's and are found to have serious limitations. Emerging new approaches to evaluate landscape dryness through the use of satellite remote sensing data, land surface modelling and data assimilation techniques are available; measuring dryness more systematically than the empirical methods. This

report try to list and describe these modern methods and datasets in order to give a clearer understanding of their characteristics and usage.

In an operational fire warning context, a temporally and spatially comprehensive dataset of soil moisture deficit at a higher resolution is required in a national scale. The very sparse ground-based soil moisture observations doesn't provide the opportunity to monitor the soil dryness at such larger scales. However, with the advances made in remote sensing of soil moisture from space, especially in the microwave spectra which has shown to be correlated to soil moisture, a detailed description of its current state is available. The remote sensing data provides the advantages of global coverage and logistics over the *in situ* observations. But these observations are only limited to the topmost soil layers (usually less than 5 cm) and doesn't give a full account of the root zone soil moisture fields. Almost complementary to the remote sensing capabilities, the land surface models gives a more detail description of the hydrological system with a sound physical basis. The land surface model are proven to be capable of producing meaningful estimates of land surface hydrologic conditions over large areas. Nevertheless, due to errors stemming from model initialisation, input parameter and meteorological forcing specifications, inadequate model physics and representativity errors from improper model resolution, the accuracy of LSMs could falter which could be proven critical for fire warnings that require higher confidence in the input soil moisture data. In order to overcome the deficiencies in LSM to some extent, remote sensing data could be ingested through advance data assimilation techniques to produce an optimal analysis of soil moisture that account for the errors in observations and model. The land surface data assimilation has shown to produce much better estimates of soil moisture states and are deemed to be an improvement over the current empirical methods employed in fire danger rating.

ACKNOWLEDGMENTS

The support of the Commonwealth of Australia through the Cooperative Research Centre program is acknowledged. We acknowledge Dr. Adam Smith, Dr. Andrew Dowdy, Dr. Huqiang Zhang and Dr. Prasanth Divakaran for their helpful comments during the preparation of this manuscript.

REFERENCES

- Al Bitar, A., Leroux, D., Kerr, Y. H., Merlin, O., Richaume, P., Sahoo, A., et al. (2012). Evaluation of SMOS soil moisture products over Continental U.S. using the SCAN/SNOTEL network. *IEEE Transactions in Geoscience and Remote Sensing*, *50*, 1572-1586.
- Albergel, C., de Rosnay, P., Gruhier, C., Munoz-Sabater, J., Hasenauer, S., Isaksen, L., et al. (2012). Evaluation of remotely sensed and modelled soil moisture products using global ground-based in situ observations. *Remote Sensing of Environment*, *118*, 215-226.
- Albergel, C., Rudiger, C., Carrer, D., Calvet, J. -C., Fritz, N., Naeimi, V., et al. (2009). An evaluation of ASCAT surface soil moisture products with in situ observations in south-western France. *Hydrology and Earth System Science*, *113*, 115-124.
- Allen, S. E. (1989). *Analysis of vegetation and other organic material*. Oxford: Blackwell Scientific Publications.
- Bergstrom, S. (1976). *Development and application of a conceptual runoff model for Scandinavian catchments*. Norrkoping: Swedish Meteorological and Hydrological Institute.
- Best, M., Pryor, M., Clark, D. B., Rooney, G. G., Essery, R. L., Menard, C. B., et al. (2011). The joint UK Land Environment Simulator (JULES), model description - Part 1: Energy and water fluxes. *Geoscience Model Development*, *4*, 677-699.
- Bogena, H. R., Huisman, J. A., Oberstdorster, C., & Vereecken, H. (2007). Evaluation of a low-cost soil water sensor for wireless network applications. *Journal of Hydrology*, *344*, 32-42.
- Bovio, G., Quaglino, A., & Nosenzo, A. (1984). Individuazione di un indice di previsione per il Pericolo di Incendi Boschivi. *Monti e Boschi Anno XXXV(4)*, (pp. 39-44).
- Brocca, L., Hasenauer, S., Lacava, T., Melone, F., Moramarco, T., Wagner, W., et al. (2011). Soil moisture estimation through ASCAT and AMSR-E sensors: an inter-comparison and validation study across Europe. *Remote Sensing of Environment*, *115*, 3390-3408.
- Burgan, R. E. (1988). *Revisions to the the 1978 Bational Fire-Danger Raing System*. Asheville: U.S. Department of Agriculture.
- Byun, H. R., & Wilhite, D. A. (1999). Objective quantification of drought severity and duration. *Journal of Climate*, *12*, 2747-2756.
- Caroll, T. R. (1981). Airborne soil moisture measurements using natural terrestrial gamma radiation. *Soil Science*, *148*, 436-447.
- Castro, F. X., Tudela, A., & Sebastia, M. T. (2003). Modelling moisture content in shrubs to predict fire risk in Catalonia (Spain). *Agricultural and Forest Meteorology*, *116*, 49-59.

- Chandler, C., Cheney, P., Thomas, P., Trabaud, L., & Williams, D. (1983). *Fire in forestry, forest fire behaviour and effects*. New York: John Wiley & Sons.
- Chen, S., Su, H., & Zhan, J. (2014). Estimating the impact of land use change on surface energy partition based on the Noah model. *Frontiers of Earth Science*, 8, 18-31.
- Chen, Y., Yang, K., Qin, J., Zhao, L., Tang, W., & Han, M. (2013). Evaluation of AMSR-E retrievals and GLDAS simulations against observations of a soil moisture network on the Tibetan Plateau. *Journal of Geophysical Research-Atmospheres*, 118, 4466-4475.
- Compton, E., & Best, M. (2011). *Impact of spatial and temporal resolution on modelled terrestrial hydrological cycle components*. Watch Project.
- Corwin, D. L., & Lesch, S. M. (2005). Characterizing soil spatial variability with apparent soil electrical conductivity I. Survey protocols. *Computers and Electronic in Agriculture*, 46, 103-133.
- Dall'Amico, J. T., Schlenz, F., Loew, A., & Mauser, W. (2012). First results of SMOS soil moisture validation in the upper Danube catchment. *IEEE Transactions in Geoscience and Remote Sensing*, 50, 1507-1516.
- de Rosnay, P., Drusch, M., Vasiljevic, D., Balsamo, G., Albergel, C., & Isaksen, L. (2012). A simplified Extended Kalman Filter for the global operational soil moisture analysis at ECMWF. *Quarterly Journal of the Royal Meteorological Society*, 139, 1199-1213.
- Desilets, D., Zreda, M., & Ferre, T. P. (2010). Nature's neutron probe: Land surface hydrology at an elusive scale with cosmic rays. *Water Resources Research*, 46(11).
- Dharssi, I., Bovis, K. J., Macpherson, B., & Jones, C. P. (2011). Operational assimilation of ASCAT surface soil wetness at the Met Office. *Hydrology and Earth System Science*, 15, 2729-2746.
- Dharssi, I., Candy, B., Bovis, K., Steinle, P., & Macpherson, B. (2013). Analysis of the linearised observation operator in a land surface data assimilation scheme for numerical weather prediction. *20th International Congress on Modelling and Simulation* (pp. 2862-2868). Adelaide: The Modelling and Simulation Society of Australia and New Zealand.
- Dharssi, I., Steinle, P., & Candy, B. (2012). *Towards a Kalman Filter based land surface data assimilation scheme for ACCESS*. Melbourne: Centre for Australian Weather and Climate Research.
- Dimitrakopoulos, A. P., & Bemmerzouk, A. M. (2003). Predicting live herbaceous moisture content from a seasonal drought index. *International Journal of Biometeorology*, 47, 73-79.
- Dimitrakopoulos, A. P., Bemmerzouk, A. M., & Mitsopoulos, I. D. (2011). Evaluation of the Canadian fire weather index system in an eastern Mediterranean environment. *Meteorological Applications*, 18, 83-93.

- Dorigo, W. A., Wagner, W., Hohensinn, R., Hahn, S., Paulik, C., Xavier, A., et al. (2011). The International Soil Moisture Network: a data hosting facility for global in situ soil moisture measurements. *Hydrology and Earth System Science*, *15*, 1675-1698.
- Dowdy, A. J., & Mills, G. A. (2012). Characteristics of lightning-attributed wildland fires in south-east Australia. *International Journal of Wildland Fire*, *21*, 521-524.
- Dowdy, A. J., Mills, G. A., Finkele, K., & de Groot, W. (2010). Index sensitivity analysis applied to the Canadian forest fire weather index and the McArthur forest fire danger index. *Meteorological Applications*, 298-312.
- Draper, C. S., Walker, J. P., Steinle, P. J., De Jeu, R. A., & Holmes, T. R. (2009). An evaluation of AMSR-E derived soil moisture over Australia. *Remote Sensing of Environment*, *113*, 703-710.
- Draper, C., Mahfouf, J. -F., Calvet, J. -C., Martin, E., & Wagner, W. (2011). Assimilation of ASCAT near-surface soil moisture into the SIM hydrological model over France. *Hydrology and Earth System Science*, *15*, 3829-3841.
- Draper, C., Reichle, R., De lannoy, G., & Liu, Q. (2012). Assimilation of passive and active microwave soil moisture retrievals. *Geophysical Research Letters*, *39*(04).
- Drusch, M., Wood, E. F., Gao, H., & Thiele, A. (2004). Soil moisture retrieval during the Southern great Plains Hydrology Experiment 1999: A comparison between experimental remote sensing data and operational products. *Water Resources Research*, *40*(02).
- Drusch, M., Wood, E., & Gao, H. (2005). Observation operators for the direct assimilation of TRMM Microwave Imager retrieved soil moisture. *Geophysical Research Letters*, *32*, L15403.
- Famiglietti, J. S., Ryu, D., Berg, A. A., Rodell, M., & Jackson, T. J. (2008). Field observations of soil moisture variability across scales. *Water Resources Research*, *44*(01).
- Field, R. D., Spessa, A. C., Aziz, N. A., Camia, A., Cantin, A., Carr, R., et al. (2014). Development of a global fire weather database for 1980-2012. *Natural Hazards Earth System Sciences Discussion*, *2*, 6555-6597.
- Finkele, K., Mills, G. A., Beard, G., & Jones, D. A. (2006). *National daily gridded soil moisture deficit and drought factors for use in prediction of forest fire danger index in Australia*. Melbourne: Australian Bureau of Meteorology.
- Frost, A. (2014, October 28). Evaluation of AWRA-L, WaterDyn and CABLE. *OzEWEX Workshop*. Canberra, ACT, Australia.
- Gao, H., Wood, E. F., Jackson, T. J., Drusch, M., & Bindlish, R. (2006). Using TRMM/TMI to retrieve surface soil moisture over the southern United States from 1998 to 2002. *Journal of hydrometeorology*, *7*, 23-38.
- Gardelin, M. (1996). *Forecasting of forest fire danger using a hydrological model*. Karlstad: Swedish Meteorological and Hydrological Institute.

- Gellie, N. J., Gibos, K. E., & Johnson, K. (2010). Relationship between severe landscape dryness and large destructive fires in Victoria. *VI International Conference on Forest Fire Research*. Coimbra, Portugal.
- Gibson, J. K., Kallberg, P., Uppala, S., Nomura, A., Hernandez, A., & Serrano, E. (1997). *ERA description*. European Centre for Medium Range Weather Forecasting. Shinfield, Reading, UK: ECMWF ERA-15 Project Report Series No. 1.
- Glowacki, T. J., Xiao, Y., & Steinle, P. (2011). Mesoscale Surface Analysis System for the Australian Domain: Design Issues, Development Status, and System Validation. *Weather and Forecasting*, *27*, 141-157.
- Godfrey, C. M., & Stensurd, D. J. (2008). Soil temperature and moisture errors in operational Eta model analyses. *Journal of Hydrometeorology*, *9*, 367-387.
- Gruhier, C., de Rosnay, P., Hasenauer, S., Holmes, T., de Jeu, R., Kerr, Y., et al. (2010). Soil moisture active and passive microwave products: inter-comparison and evaluation over a Sahelian site. *Hydrology and Earth System Science*, *14*, 141-156.
- Guha, A., & Lakshmi, V. (2002). Sensitivity, spatial heterogeneity, and scaling of C-band microwave brightness temperatures for land hydrological studies. *IEEE Transaction on Geoscience and Remote Sensing*, *40*, 2626-2635.
- Hanks, R. J., & Ashcroft, G. L. (1986). *Applied soil physics*. Berlin: Springer-Verlag.
- Heikinheimo, M., Vanalainen, A., & Tourula, T. (1998). A soil moisture index for the assessment of forest fire potential in the boreal zone. *Proceedings of the International Symposium on Applied Agrometeorology and Agroclimatology*. Volos, Greece.
- Henderson-Sellers, A., Pitman, A. J., Love, P. K., Irannejad, P., & Chen, T. H. (1995). The Project for Inter-comparison of Land-surface Parameterization Schemes (PILPS): Phase 2 and 3. *Bulletin of American Meteorological Society*, *76*, 489-503.
- Hollinger, J. P., Peirce, J. L., & Poe, G. A. (1990). SSM/I instrument evaluation. *IEEE Transaction on Geoscience and Remote Sensing*, *28*, 489-503.
- Imaoka, K., Kachi, M., Fujii, H., Murakami, H., Hori, M., Ono, A., et al. (2010). Global Change Observation Mission (GCOM) for monitoring carbon, water cycle and climate change. *Proceedings of IEEE*, *98*, 717-734.
- Jackson, T. J., & Schmugge, T. J. (1995). Surface soil moisture measurements with microwave radiometry. *Acta Astronautica*, *35*, 477-482.
- Jackson, T. J., Hsu, A. Y., & O'Neill, P. E. (2002). Surface soil moisture retrieval mapping using high-frequency microwave satellite observations in the Southern Great Plains. *Journal of Hydrometeorology*, *3*, 688-699.
- Jackson, T. J., Le Vine, D. M., Hsu, A. Y., Oldak, A., Starks, P. J., Swift, C. T., et al. (1999). Soil moisture mapping at regional scales using microwave radiometry: The Southern Great Plains hydrology experiment. *IEEE Transactions on Geoscience and Remote Sensing*, *37*, 2136-2151.
- Jackson, T. J., Schmugge, T. J., & Engman, E. T. (1996). Remote sensing applications to hydrology: Soil moisture. *Hydrological Science*, *41*, 517-530.

- Janis, M. J., Johnson, M. B., & Forthun, G. (2002). Near-real time mapping of Keetch-Byram drought index in the south-eastern United States. *International Journal of Wildland Fire*, *11*, 281-289.
- Jones, D. A., Wang, W., & Fawcett, R. (2009). *Climate data for the Australian Water Availability Project: Final milestone report*. Melbourne: National Climate Centre, Bureau of Meteorology.
- Kalnay, E., Kanamitsu, M., Kistler, R., Collins, W., Deaven, D., Gandin, L., et al. (1996). The NCEP/NCAR 40-Year Reanalysis Project. *Bulletin of American Meteorological Society*, *77*, 437-471.
- Keetch, J. J., & Byram, G. M. (1968). *A drought index for forest fire control*. Asheville: U.S. Department of Agriculture and Forest Service.
- King, A. D., Alexander, L. V., & Donat, M. G. (2013). The efficacy of using gridded data to examine extreme rainfall characteristics: A case study for Australia. *International Journal of Climatology*, *33*, 2376-2387.
- Koster, R. D., Guo, Z., Yang, R., Dirmeyer, P. A., Mitchell, K., & Puma, M. J. (2009). On the nature of soil moisture in land surface models. *Journal of Climate*, *22*, 4322-4335.
- Kowalczyk, E., Stevens, L., Law, R., Dix, M., Wang, Y., Harman, I., et al. (2013). The land surface model component of ACCESS: description and impact on the simulated surface climatology. *Australian Meteorological and Oceanographic Journal*, *63*, 65-82.
- Lacava, T., Matgen, P., Brocca, L., Bittelli, M., Pergola, N., Moramarco, T., et al. (2012). A first assessment of the SMOS soil moisture product with in-situ and modelled data in Italy and Luxemburg. *IEEE Transactions in Geoscience Remote Sensing*, *50*, 1612-1622.
- Lakshmi, V. (1998). Special sensor microwave imager data in field experiments: FIFE-1987. *International Journal of Remote Sensing*, *19*, 481-505.
- Lakshmi, V. (2013). Remote sensing of soil moisture. *Soil Science*, 2013.
- Lambot, S., Weihermuller, L., Huisman, J. A., Vereecken, H., Vanclooster, M., & Slob, E. C. (2006). Analysis of air-launched ground-penetrating radar techniques to measure the soil surface water content. *Water Resource research*, *42*(11).
- Li, L., Gaiser, P., Jackson, T. J., Bindlish, R., & Du, J. (2007). Windsat soil moisture algorithm and validation. *Proceedings of the International Geoscience and Remote Sensing Symposium*, (pp. 1188-1191). Barcelona, Spain.
- Lindstrom, G., Johansson, B., Persson, M., Gardelin, M., & Bergstrom, S. (1997). Development and test of the distributed HBV-96 model. *Journal of hydrology*, *201*, 272-288.
- Luke, R. H., & McArthur, A. G. (1978). *Bushfires in Australia*. Canberra, Australia: Australian Government Publication Service.
- McArthur, A. G. (1967). *Fire behaviour in Eucalypt forest*. Australian Commonwealth Forestry and Timber Bureau Leaflet.

- Mitchell, K. E., & et, a. (2004). The multi-institution North American Land Data Assimilation System (NLDAS) project: Utilizing multiple GCIP products and partners in a continental distributed hydrological modelling system. *Journal of Geophysical Research*, 109(07).
- Mittelbach, H., Lehner, I., & Seneviratne, S. I. (2012). Comparison of four soil moisture sensor types under field conditions in Switzerland. *Journal of Hydrology*, 430, 39-49.
- Mount, A. B. (1972). *The derivation and testing of a soil dryness index using runoff data*. Hobart: Tasmanian Forestry Commission.
- Nichols, S., Zhang, Y., & Ahmad, A. (2011). Review and evaluation of remote sensing methods for soil-moisture estimation. *Journal of Photonics for Energy*, 2, 028001-17.
- Niu, G.-Y., Yang, Z.-L., Mitchell, K. E., Chen, F., Ek, M. B., Barlage, M., et al. (2011). The community Noah land surface model with multiparameterization options (Noah-MP): 1. Model description and evaluation with local-scale measurements. *Journal of Geophysical Research: Atmospheres*, 116, 2156-2202.
- Njoku, E. G., & Chan, S. K. (2006). Vegetation and surface roughness effects on AMSR-E land observations. *Remote Sensing of Environment*, 100, 190-199.
- Njoku, E. G., Rague, B., & Fleming, K. (1998). *The Nimbus-7 SMMR Pathfinder brightness temperature dataset*. Pasadena, California: Jet Propulsion Laboratory Publication.
- Owe, M., De Jeu, R. A., & Holmes, T. (2008). Multi-sensor historical climatology of satellite-derived global land surface moisture. *Journal of Geophysical Research*, 113(01).
- Paloscia, S., Macelloni, G., Santi, E., & Koike, T. (2001). A multi-frequency algorithm for the retrieval of soil moisture on a large scale using microwave data from SMMR and SSM/I satellites. *IEEE Transactions on Geoscience and Remote Sensing*, 39, 1655-1661.
- Paulik, C., Dorigo, W., Wagner, W., & Kidd, R. (2014). Validation of the ASCAT soil water index using in situ data from the International Soil Moisture Network. *International Journal of Applied Earth Observation and Geoinformation*, 30, 1-8.
- Price, J. C. (1982). On the use of satellite data to infer surface fluxes at meteorological scales. *Journal of Applied Meteorology*, 21, 1111-1122.
- Quesney, A., Le Hegarat-Masclé, S., Taconet, O., Vidal-Madjar, D., Wigneron, J. P., Loumagne, C., et al. (2000). Estimation of watershed soil moisture index from ERS/SAR data. *Remote Sensing of Environment*, 72, 290-303.
- Raupach, M. R., Briggs, P. R., Haverd, V., King, E. A., Paget, M., & Trudinger, C. M. (2009). *Australian Water Availability Project (AWAP): Final report for phase 3*. Melbourne: CAWCR Tech Report No. 013.
- Reichle, R., & Koster, R. (2004). Bias reduction in short records of satellite soil moisture. *Geophysical Research Letters*, 31, L19501.

- Reichle, R., Koster, R. D., Dong, J., & Berg, A. A. (2004). Global soil moisture from satellite observations, land surface models, and ground data: Implications for data assimilation. *Journal of Hydrometeorology*, 5, 430-442.
- Robinson, D. A., Campbell, C. S., Hopmans, J. W., Hornbuckle, B. K., Jones, S. B., Knight, R., et al. (2008). Soil moisture measurement for ecological and hydrological watershed-scale observatories: A review. *Vadose Zone Journal*, 7, 358-389.
- Robinson, D. A., Jones, S. B., Wraith, J. A., Or, D., & Friedman, S. P. (2003). A review of advances in dielectric and electrical conductivity measurement in soils using time domain reflectometry. *Vadose Zone Journal*, 2, 444-475.
- Robock, A., Vinnikov, K. Y., Srinivasan, G., Entin, J. K., Hollinger, S. E., Speranskaya, N. A., et al. (2000). The Global Soil Moisture Data Bank. *Bulletin of American Meteorological Society*, 81, 1281-1299.
- Rüdiger, C., Hancock, G. R., Hemakumara, H. M., Jacobs, B., Kalma, J. D., Martinez, C., et al. (2007). Goulburn River Experimental Catchment Data Set. *Water Resources Research*, 43, W10403.
- Rudiger, C., Walker, J. P., Kaihotsu, I., Fujii, H., Yee, M., & Monerris, A. (2013). A first glance at AMSR2 soil moisture observations across Australia. *Satellite Soil Moisture Validation & Application Workshop*. Frascati, Italy.
- Rudiger, C., Walker, J. P., Kaihotsu, I., Fujii, H., Yee, M., & Monerris, A. (2013, July 1-3). A first glance at AMSR2 soil moisture observations across Australia. *Satellite Soil Moisture Validation & Application Workshop*. Frascati, Lazio, Italy: ESA/ESRIN.
- Samouelian, A., Cousin, I., Tabbagh, A., Bruand, A., & Richard, G. (2005). Electrical resistivity survey in soil science: A review. *Soil Tillage Research*, 83, 173-193.
- Sanchez, N., Martinez-Fernandez, J., & Perez-Gutierrez, C. (2012). Validation of SMOS L2 soil moisture data in REMEDHUS network (Spain). *IEEE Transactions in Geoscience and Remote Sensing*, 50, 1602-1611.
- Smith, A. B. (2014). *Soil moisture monitoring with ground-based gravity data*. Australia: University of Melbourne.
- Smith, A. B., Walker, J. P., Western, A. W., Young, R. I., Ellett, K. M., Pipunic, R. C., et al. (2012). The Murrumbidgee Soil Moisture Monitoring Network data set. *Water Resources Research*, 48(07).
- Uppala, S. M., Kallberg, P. W., Simmons, A. J., Andrea, U., Bechtold, V. C., Fiorino, M., et al. (2005). The ERA-40 re-analysis. *Quarterly Journal of Royal Meteorological Society*, 131, 2961-3012.
- Vachaud, G., Royer, J. M., & Cooper, J. D. (1977). Comparison of methods of calibration of a neutron probe by gravimetry or neutron capture model. *Journal of Hydrology*, 34, 343-356.
- Valente, A., Morais, R., Tuli, A., Hopmans, J. W., & Kluitenberg, G. J. (2006). Multi-functional probe for small-scale simultaneous measurements of soil thermal properties, water content, and electrical conductivity. *Sensors Actuators A*, 132, 70-77.

- van der Velde, R., Salama, M. S., Pellarin, T., Ofwono, M., Ma, Y., & Su, Z. (2014). Long term soil moisture mapping over the Tibetan Plateau using Special Sensor Microwave / Imager. *Hydrology and Earth System Sciences*, 18, 1323-1337.
- van Dijk, A. I. (2010). *The Australian Water Resources Assessment System*. Canberra: Technical report 3. Landscape model (version 0.5) technical description WIRADA technical report, CSIRO Water for a Healthy Country Flagship.
- van Wagner, C. E. (1987). *Development and structure of the Canadian Forest Fire Weather Index System*. Ottawa: Canadian Forestry Service.
- Vereecken, H., Huisman, J. A., Bogaen, H., Vanderborght, J., Vrugt, J. A., & Hopmans, J. W. (2008). On the value of soil moisture measurements in vadose zone hydrology: A review. *Water Resources Research*, 44, W00D06.
- Viegas, D. X., Pinol, J., Viegas, M. T., & Ogaya, R. (2001). Estimating live fine fuel moisture content using meteorologically-based indexes. *International Journal of Wildland Fire*, 10, 223-240.
- Viegas, D., Viegas, P., & Ferreira, A. (1992). Moisture content of fine forest fuels and fire occurrence in central Portugal. *International Journal of Wildland Fire*, 2, 69-85.
- Vinodkumar, Chandrasekar, A., Alapaty, A., & Niyogi, D. (2009). Assessment of data assimilation approaches for the simulation of monsoon depression over the Indian monsoon region. *Boundary Layer Meteorology*, 133, 343-366.
- Wagner, W., Naeimi, V., Scipal, K., Jeu, R., & Martinez-Fernandez, J. (2007). Soil moisture from operational meteorological satellites. *Hydrogeology Journal*, 15, 121-131.
- Walker, J. P., & Houser, P. R. (2004). Requirements of a Global Near-Surface Soil Moisture Satellite Mission: Accuracy, Repeat Time, and Spatial Resolution. *Advances in Water Resources*, 27, 785-801.
- Walker, J. P., Beringer, J., Rudiger, C., & Daly, E. (2012). *Towards global water and energy balance monitoring using GCOM-W1 in the Australian Murray Darling Basin*. Tokyo: Joint PI Workshop of Global Environment Observation Mission.
- Wen, J., Jackson, T. J., Bindlish, R., Hsun, A. Y., & Su, Z. B. (6). Retrieval of soil moisture and vegetation water content using SSM/I data over a corn and soybean region. *Journal of Hydrometeorology*, 6, 854-863.
- Western, A. W., Grayson, R. B., & Blöschl, G. (2002). Scaling of soil moisture - A hydrological perspective. *Annual review of Earth and Planetary Science*, 30, 149-180.
- Williams, K., & Clark, D. (2014). *Disaggregation of daily data in JULES*. Exeter: UK Met Office.
- Willis, C., van Wilgen, B., Tolhurst, K., Everson, C., D'Abreton, P., Pero, L., et al. (2001). *Development of a national fire danger rating system for South Africa*. Pretoria: Department of Water Affairs and Forestry.

APPENDIX A: THEORETICAL BACKGROUND ON MICROWAVE REMOTE SENSING

Microwave radiance measured by a satellite sensor is a sum of the land surface emission and cumulative contribution from the atmospheric layers. This can be written in the form of a rather simplified equation as:

$$L = \mathcal{E}_s^P B_\lambda(T_s)\tau_s + \sum \mathcal{E}_a^P B_\lambda(T_a)\tau_a \quad (10)$$

where \mathcal{E}^P is the emissivity of the medium (surface/atmospheric layer), $B_\lambda(T)$ is the Planck function, λ is the wavelength sensed by the instrument, and τ is the atmospheric transmittance. The subscripts s and a denotes the surface and atmospheric contributions and the superscript P denotes the polarization of the microwave radiation (*i.e.*, either horizontal (H) or vertical (V) polarized). The summation in the second term on right hand side indicates the sum of radiance emitted by each layer of the atmosphere with a physical temperature T_a .

For land surface, the brightness temperature is related to the physical temperature as:

$$T_B^P \cong \mathcal{E}_s^P T_s \quad (11)$$

The surface emissivity is given by:

$$\mathcal{E}_s^P = 1 - \rho_s^P \quad (12)$$

where ρ_s^P is the surface reflectivity. For a smooth surface and a medium of uniform dielectric constant, the expressions for reflectivity at horizontal and vertical polarizations are given by Fresnel's expressions:

$$\rho_s^V = \left| \frac{\epsilon_r \cos\theta - \sqrt{\epsilon_r - \sin^2\theta}}{\epsilon_r \cos\theta + \sqrt{\epsilon_r - \sin^2\theta}} \right|^2 \quad (13)$$

$$\rho_s^H = \left| \frac{\cos\theta - \sqrt{\epsilon_r - \sin^2\theta}}{\cos\theta + \sqrt{\epsilon_r - \sin^2\theta}} \right|^2 \quad (14)$$

where θ is the incidence angle and ϵ_r is the complex dielectric constant of the medium.

Since water has a higher ϵ_r compared to soil, an increase in soil moisture content of the soil increases the ϵ_r of soil layer. This lowers the surface emissivity and which inturn results in a corresponding decrease of observed brightness temperature. The absolute

magnitude of the soil emissivity is lower at H polarization than at V polarization, though the sensitivity to changes in soil moisture is considerably greater at H polarization than at V polarization (Owe *et al.*, 2008)

